Table 3 | Quantitative PCR data summary of anterior cingulate cortex (ACC) genes in BPD or MDD that showed altered expression compared to the control group.

Symbol	Gene name	BPD vs. Control				MDD vs. Control			
		Microarray % change	Unadjusted *p*-value	qPCR % change	Unadjusted *p*-value	Microarray % change Cohort B	Unadjusted *p*-value	qPCR % change	Unadjusted *p*-value
SST	Somatostatin	22.1	5.4 E−05**	10.1	$p > 0.05$	−6.5	0.108	NT	NT
GPRC5B	G protein-coupled receptor C−5−B	24.6	6.13E−06**	46.8	$p < 0.05$	−30.3	0.00004**	−54.0	$p < 0.01$
INPP1	Inositol polyphosphate-1-phosphatase	24.9	9.4E−06**	21.7	$p < 0.05$	−7.4	0.04372	NT	NT
NPY	Neuropeptide Y	33.0	1.48E−06**	37.6	$p < 0.05$	3.6	0.54313	NT	NT
GPR37	G protein-coupled receptor 37	38.3	9.46E−08**	54.1	$p < 0.05$	−27.0	0.00003**	−62.7	$p < 0.05$
RGS20	Regulator of G-protein signaling 20	15.6	0.005	NT	NT	−29.2#	5.85E−06**#	−36.9	$p < 0.01$
PPP1R3C	Protein phosphatase 1 regulatory subunit 3C	−15.4	0.0005	NT	NT	−21.4	0.00006**	−46.1	$p < 0.01$

These genes selected for qPCR analyses met the criteria of false discovery rate multiple testing correction at the level of accepting 5% false positives and percentage change greater than 20% in the anterior cingulate cortex microarray results in Cohort A for BPD, and in Cohort B for MDD. The qPCR analyses were run for seven representative GPLS selected from ligand peptides, GPCRs, and G protein regulators.

NT, not tested by qPCR as did not meet criteria of 20% change and passing FDR by microarray.

***Indicates a gene that passed FDR.*

#RGS20 values shown are for Cohort A.

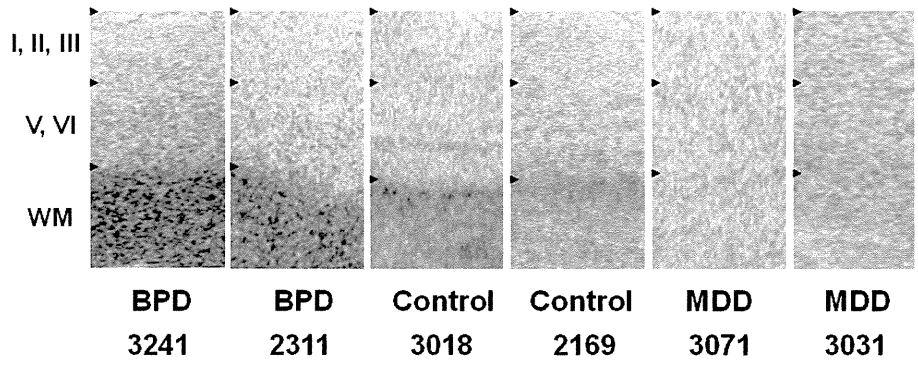

FIGURE 2 | *In situ* hybridization images of GPR37 mRNA in representative BPD, MDD and control subjects. GPR37 mRNA is preferentially expressed in subcortical white matter. Among six layers of cortical gray matter, GPR37 expression in deeper layers (V–VI) is relatively higher than in superficial layer (I–III). Expression levels in GPR37 is increased in the BPD subjects, and decreased in MDD subjects in subcortical white matter in anterior cingulate cortex tissue, compared to control subjects. WM, Subcortical white matter; BPD, Bipolar disorder; MDD, Major depressive disorder.

phosphatidylinositol signaling pathways. The following pattern of alterations in GPLS were observed:

(1) Transcriptional levels of molecules acting as negative regulators in cAMP signaling pathways are increased in BPD and decreased in MDD, which may compensate for the activated cAMP signaling activity in BPD and the blunted cAMP signaling activity in MDD,

(2) Expression of PRKCB1, ITPR1, INPP5F, and ITPKB were altered in MDD, which may reflect functional impairments of G_q and PLC-beta in the disorder,

(3) Expression of INPP1 and phosphatidylinositol 3-kinases were altered in BPD suggesting that these molecules may be involved in both the pathophysiology and the mechanism(s) of action of lithium treatment of BPD, and
(4) Two orphan GPCR genes, GPRC5B and GPR37, showed significant increases in ACC of BPD, and decreases in ACC and DLPFC of MDD.

ORPHAN G PROTEIN-COUPLED RECEPTORS

Among all GPCRs, the most consistent differential expression patterns were observed for GPRC5B and GPR37. GPRC5B was significantly increased in ACC and DLPFC of BPD, while significantly decreased in ACC and DLPFC of MDD patients. GPR37 was significantly increased in ACC of BPD, and significantly decreased in ACC and DLPFC of MDD patients. The consistent cortical alterations of GPRC5B and GPR37 expression observed in MDD patients suggest a role of these genes in the pathophysiology of MDD. So far, these two orphan GPCRs have not been highlighted as candidate susceptible genes for BPD and MDD, however previous microarray data supports decrease of both GPRC5B and GPR37 expressions in MDD patients (Aston et al., 2005). Our microarray data strongly suggests these genes might be involved in the pathophysiology of the disorders. GPR37 and GPRC5B are both implicated in Parkinson's disease (Marazziti et al., 2009, 2011), which has depression as one premorbid indicator, possibly concomitant with brain neurodegenerative processes.

GPR37 appears to facilitate dopamine neurotransmission, and reductions in brain GPR37 leads to behavioral alterations in conditioned place preferences to reinforcements such as cocaine or amphetamine (Marazziti et al., 2011). GPR37 (Class A receptor) contains a large extracellular domain which led to speculations that the ligand of this receptor may be a protein rather than a peptide (Leng et al., 1999). GPR37 is predominantly expressed in the brain (Zeng et al., 1997; Marazziti et al., 1998; Leng et al., 1999), especially in glial cells of the fiber tracts, Purkinje cells in cerebellum, neuronal cells in hippocampus CA3 region and substantianigra (Zeng et al., 1997; Imai et al., 2001). GPR37 has been shown to be involved in the dopaminergic system (Imai et al., 2001, 2002; Marazziti et al., 2004). GPR37 is also called Pael receptor (PAELR). Unfolded PAELR is a substrate of E3 ubiquitin ligase Parkin, and accumulation of Pael-R in the endoplasmic reticulum (ER) of dopaminergic neurons is considered to induce ER stress leading to neurodegeneration in Parkinson disease (Imai et al., 2002). Gpr37$^{-/-}$ mice shows reduced striatal dopamine content and enhanced amphetamine sensitivity (Marazziti et al., 2004). Our ISH data suggest that the predominant expression of GPR37 mRNA in ACC occurred mainly in subcortical white matter. GPR37 is a substrate of parkin (PARK2), and its insoluble aggregates accumulate in brain tissue samples of Parkinson's disease patients, AKA PaelR (Marazziti et al., 2009).

GPRC5B is phylogenetically classified into a type C GPCR, however, in contrast to other type C genes, GPRC5B has a short N terminal domain (Brauner-Osborne and Krogsgaard-Larsen, 2000). QPCR based expression analysis shows GPRC5B is predominantly expressed in brain, with most abundant expression in neuronal cells of caudate, putamen, substantia nigra, thalamus and hippocampus and glial cells of the fiber tracts (Brauner-Osborne and Krogsgaard-Larsen, 2000; Robbins et al., 2002). Behavioral abnormalities exist in GPRC5B knock-outs, decreased spontaneous locomotor activity, and decreased responses to a new environment (Sano et al., 2011).

The expression patterns of GPRC5B and GPR37 suggest that both of these orphan GPCRs may be involved in various cellular functional activities in the brain including neuronal and glial cells. Functional characterization of GPRC5B and GPR37 may provide new insights into the pathophysiology of mood disorder, and potential novel strategies for developing methods for diagnoses and treatment of the disorders.

There are limitations to this post-mortem study of GPLS pathway expression. We conducted seven qPCR validations of genes that passed FDR, and although a small number, those genes did represent large enough percent fold changes to validate by qPCR. Other technologies could be used that are less costly, such as Nanostring or Fluidigm for additional validation studies, which are now being conducted on larger sample sizes. In addition, we do not have confirmed toxicological analysis of all drugs of abuse and therapeutic levels to rule out these effects in explaining case—control expression differences. Finally, we are aware that small residual agonal effects might exist that are not corrected in this analysis, however we did confirm that the present data presented in **Table 2**, was not due to the effects of age or pH on gene expression.

SUMMARY

This study highlights transcript profile differences in GPLS pathways in both BPD and MDD. Since sample sizes were low, we also used a second independent cohort in the case of MDD gene expression to check concordance. We relied upon duplicate microarray analysis at independent laboratories, and used gene expression values that were significantly correlated between sites, and employed FDR to select genes to advance for qPCR experimental validations.

The disturbances observed in cAMP- and phosphatidylinositol- pathway regulation may be due to differential activation of individual GPCRs and individual differences in ligand- receptor sensitivity, suggesting that functional and genetic characterization of these candidate genes may provide further understanding of the pathophysiology of mood disorders. Further studies will also be required to investigate additional GPCR signaling pathway features such as receptor phosphorylation, beta-arrestin recruitment, receptor desensitization, and internalization, and beta-gamma mediated signaling. The results of the present study suggest that future functional activity studies of the GPLS pathways would elucidate the relationship of the observed transcript changes to protein levels and functional outcomes in mood disorders.

ACKNOWLEDGMENTS

Authors of this manuscript were members of the Silvio O. Conte Center for "Genomic Studies in Bipolar and Major Depression" which was supported by the NIMH grant P50 MH60398, and the Pritzker Neuropsychiatric Disorders Research Consortium currently supported by the Pritzker Neuropsychiatric Disorders

Research Fund L.L.C. A shared intellectual property agreement exists between the Fund and all the universities involved, in order to encourage the development of appropriate findings for research and clinical applications. The academic and philanthropic entities involved in this research program are jointly filing patent applications related to the present findings. This project is also supported by Della Martin Foundation (UCI), William Lion Penzner Foundation (UCI), and the NIMH MH42251 (Stanley J. Watson and Huda Akil), and MH085801 (Marquis P. Vawter) and MH099440 (Marquis P. Vawter). We appreciate the assistance of Preston Cartagena, Psy.D., David Walsh, Ph.D., and Richard Stein, Ph.D. of the University of California, Irvine (UCI) Brain Repository for their contributions to post-mortem clinical characterization of subjects, and Kathleen Burke (UCI), Claudia M. Cervantes (UCI) for procurement of brain tissue, as well as Chief Deputy Coroner Jacque Berndt, and the staff of Orange County Coroners' Office. Neuropathological evaluation of the post-mortem brains was performed by F. Warren Lovell, M.D. Tissue specimens were processed and stored at the Human Brain and Spinal Fluid Resource Center, Veteran's Medical Center, Los Angeles under the direction of Wallace W. Tourtellotte, M.D., Ph.D. We also appreciate the technical contributions of Ling Shao, Kevin M. Overman, Sharon M. Burke (U Mich), as well as critical reviews by Hans-Peter Nothacker (UCI, Department of Pharmacology) and Blynn Bunney (UCI).

SUPPLEMENTARY MATERIAL

The Supplementary Material for this article can be found online at: http://www.frontiersin.org/journal/10.3389/fgene.2013.00297/abstract.

REFERENCES

Agam, G., Shaltiel, G., Kozlovsky, N., Shimon, H., Belmaker, R. H., and Shatiel, G. (2003). Lithium inhibitable enzymes in postmortem brain of bipolar patients. *J. Psychiatr. Res.* 37, 433–442. doi: 10.1016/S0022-3956(03)00044-X

Aston, C., Jiang, L., and Sokolov, B. P. (2005). Transcriptional profiling reveals evidence for signaling and oligodendroglial abnormalities in the temporal cortex from patients with major depressive disorder. *Mol. Psychiatry.* 10, 309–322. doi: 10.1038/sj.mp.4001565

Atz, M., Walsh, D., Cartagena, P., Li, J., Evans, S., Choudary, P., et al. (2007). Methodological considerations for gene expression profiling of human brain. *J. Neurosci. Methods* 163, 295–309. doi: 10.1016/j.jneumeth.2007.03.022

Brauner-Osborne, H., and Krogsgaard-Larsen, P. (2000). Sequence and expression pattern of a novel human orphan G-protein-coupled receptor, GPRC5B, a family C receptor with a short amino-terminal domain. *Genomics* 65, 121–128. doi: 10.1006/geno.2000.6164

Caberlotto, L., and Hurd, Y. L. (2001). Neuropeptide Y Y(1) and Y(2) receptor mRNA expression in the prefrontal cortex of psychiatric subjects. Relationship of Y(2) subtype to suicidal behavior. *Neuropsychopharmacology* 25, 91–97. doi: 10.1016/S0893-133X(00)00231-1

Carvajal, C., Dumont, Y., and Quirion, R. (2006). Neuropeptide y: role in emotion and alcohol dependence. *CNS Neurol. Disord. Drug Targets* 5, 181–195. doi: 10.2174/187152706776359592

Chang, A., Li, P. P., and Warsh, J. J. (2003). cAMP-Dependent protein kinase (PKA) subunit mRNA levels in postmortem brain from patients with bipolar affective disorder (BD). *Brain Res. Mol. Brain Res.* 116, 27–37. doi: 10.1016/S0169-328X(03)00211-0

Choudary, P. V., Molnar, M., Evans, S. J., Tomita, H., Li, J. Z., Vawter, M. P., et al. (2005). Altered cortical glutamatergic and GABAergic signal transmission with glial involvement in depression. *Proc. Natl. Acad. Sci. U.S.A.* 102, 15653–15658. doi: 10.1073/pnas.0507901102

Dai, M., Wang, P., Boyd, A. D., Kostov, G., Athey, B., Jones, E. G., et al. (2005). Evolving gene/transcript definitions significantly alter the interpretation of GeneChip data. *Nucleic Acids Res.* 33, e175. doi: 10.1093/nar/gni179

Donati, R. J., and Rasenick, M. M. (2003). G protein signaling and the molecular basis of antidepressant action. *Life Sci.* 73, 1–17. doi: 10.1016/S0024-3205(03)00249-2

Dwivedi, Y., Agrawal, A. K., Rizavi, H. S., and Pandey, G. N. (2002). Antidepressants reduce phosphoinositide-specific phospholipase C (PI-PLC) activity and the mRNA and protein expression of selective PLC beta 1 isozyme in rat brain. *Neuropharmacology* 43, 1269–1279. doi: 10.1016/S0028-3908(02)00253-8

Dwivedi, Y., Mondal, A. C., Shukla, P. K., Rizavi, H. S., and Lyons, J. (2004). Altered protein kinase a in brain of learned helpless rats: effects of acute and repeated stress. *Biol. Psychiatry* 56, 30–40. doi: 10.1016/j.biopsych.2004.03.018

Elhwuegi, A. S. (2004). Central monoamines and their role in major depression. *Prog. Neuropsychopharmacol. Biol. Psychiatry* 28, 435–451. doi: 10.1016/j.pnpbp.2003.11.018

Escriba, P. V., Ozaita, A., and Garcia-Sevilla, J. A. (2004). Increased mRNA expression of alpha2A-adrenoceptors, serotonin receptors and mu-opioid receptors in the brains of suicide victims. *Neuropsychopharmacology* 29, 1512–1521. doi: 10.1038/sj.npp.1300459

Evans, S. J., Choudary, P. V., Neal, C. R., Li, J. Z., Vawter, M. P., Tomita, H., et al. (2004). Dysregulation of the fibroblast growth factor system in major depression. *Proc. Natl. Acad. Sci. U.S.A.* 101, 15506–15511. doi: 10.1073/pnas.0406788101

Frazier, J. A., Ahn, M. S., DeJong, S., Bent, E. K., Breeze, J. L., and Giuliano, A. J. (2005). Magnetic resonance imaging studies in early-onset bipolar disorder: a critical review. *Harv. Rev. Psychiatry* 13, 125–140. doi: 10.1080/10673220591003597

Frey, R., Metzler, D., Fischer, P., Heiden, A., Scharfetter, J., Moser, E., et al. (1998). Myo-inositol in depressive and healthy subjects determined by frontal 1H-magnetic resonance spectroscopy at 1.5 tesla. *J. Psychiatr. Res.* 32, 411–420. doi: 10.1016/S0022-3956(98)00033-8

Friedman, E., and Wang, H. Y. (1996). Receptor-mediated activation of G proteins is increased in postmortem brains of bipolar affective disorder subjects. *J. Neurochem.* 67, 1145–1152. doi: 10.1046/j.1471-4159.1996.67031145.x

Gould, T. D., and Manji, H. K. (2002). Signaling networks in the pathophysiology and treatment of mood disorders. *J. Psychosom. Res.* 53, 687–697. doi: 10.1016/S0022-3999(02)00426-9

Gurevich, I., Tamir, H., Arango, V., Dwork, A. J., Mann, J. J., and Schmauss, C. (2002). Altered editing of serotonin 2C receptor pre-mRNA in the prefrontal cortex of depressed suicide victims. *Neuron* 34, 349–356. doi: 10.1016/S0896-6273(02)00660-8

Harrison, P. J. (2002). The neuropathology of primary mood disorder. *Brain* 125(Pt 7), 1428–1449. doi: 10.1093/brain/awf149

Harwood, A. J. (2005). Lithium and bipolar mood disorder: the inositol-depletion hypothesis revisited. *Mol. Psychiatry* 10, 117–126. doi: 10.1038/sj.mp.4001618

Imai, Y., Soda, M., Hatakeyama, S., Akagi, T., Hashikawa, T., Nakayama, K. I., et al. (2002). CHIP is associated with Parkin, a gene responsible for familial Parkinson's disease, and enhances its ubiquitin ligase activity. *Mol. Cell* 10, 55–67. doi: 10.1016/S1097-2765(02)00583-X

Imai, Y., Soda, M., Inoue, H., Hattori, N., Mizuno, Y., and Takahashi, R. (2001). An unfolded putative transmembrane polypeptide, which can lead to endoplasmic reticulum stress, is a substrate of Parkin. *Cell* 105, 891–902. doi: 10.1016/S0092-8674(01)00407-X

Iwamoto, K., Kakiuchi, C., Bundo, M., Ikeda, K., and Kato, T. (2004). Molecular characterization of bipolar disorder by comparing gene expression profiles of postmortem brains of major mental disorders. *Mol. Psychiatry.* 9, 406–416. doi: 10.1038/sj.mp.4001437

Jope, R. S., Song, L., Li, P. P., Young, L. T., Kish, S. J., Pacheco, M. A., et al. (1996). The phosphoinositide signal transduction system is impaired in bipolar affective disorder brain. *J. Neurochem.* 66, 2402–2409.

Karege, F., Bovier, P., Rudolph, W., and Gaillard, J. M. (1996). Platelet phosphoinositide signaling system: an overstimulated pathway in depression. *Biol. Psychiatry* 39, 697–702. doi: 10.1016/0006-3223(95)00187-5

Kim, S., and Webster, M. J. (2010). Correlation analysis between genome-wide expression profiles and cytoarchitectural abnormalities in the prefrontal cortex of psychiatric disorders. *Mol. Psychiatry* 15, 326–336. doi: 10.1038/mp.2008.99

Konradi, C., Eaton, M., MacDonald, M. L., Walsh, J., Benes, F. M., and Heckers, S. (2004). Molecular evidence for mitochondrial dysfunction in

bipolar disorder. *Arch. Gen. Psychiatry* 61, 300–308. doi: 10.1001/archpsyc.61.3.300

Kuromitsu, J., Yokoi, A., Kawai, T., Nagasu, T., Aizawa, T., Haga, S., et al. (2001). Reduced neuropeptide Y mRNA levels in the frontal cortex of people with schizophrenia and bipolar disorder. *Gene Expr. Patterns* 1, 17–21. doi: 10.1016/S1567-133X(01)00003-5

Leng, N., Gu, G., Simerly, R. B., and Spindel, E. R. (1999). Molecular cloning and characterization of two putative G protein-coupled receptors which are highly expressed in the central nervous system. *Brain Res. Mol. Brain Res.* 69, 73–83. doi: 10.1016/S0169-328X(99)00092-3

Li, J. Z., Vawter, M. P., Walsh, D. M., Tomita, H., Evans, S. J., Choudary, P. V., et al. (2004). Systematic changes in gene expression in postmortem human brains associated with tissue pH and terminal medical conditions. *Hum. Mol. Genet.* 13, 609–616. doi: 10.1093/hmg/ddh065

Lieb, K., Treffurth, Y., Berger, M., and Fiebich, B. L. (2002). Substance P and affective disorders: new treatment opportunities by neurokinin 1 receptor antagonists? *Neuropsychobiology* 45(Suppl. 1), 2–6. doi: 10.1159/000049254

Lopez-Figueroa, A. L., Norton, C. S., Lopez-Figueroa, M. O., Armellini-Dodel, D., Burke, S., Akil, H., et al. (2004). Serotonin 5-HT1A, 5-HT1B, and 5-HT2A receptor mRNA expression in subjects with major depression, bipolar disorder, and schizophrenia. *Biol. Psychiatry* 55, 225–233. doi: 10.1016/j.biopsych.2003.09.017

Marazziti, D., Di Pietro, C., Golini, E., Mandillo, S., Matteoni, R., and Tocchini-Valentini, G. P. (2009). Macroautophagy of the GPR37 orphan receptor and Parkinson disease-associated neurodegeneration. *Autophagy* 5, 741–742. doi: 10.4161/auto.5.5.8700

Marazziti, D., Di Pietro, C., Mandillo, S., Golini, E., Matteoni, R., and Tocchini-Valentini, G. P. (2011). Absence of the GPR37/PAEL receptor impairs striatal Akt and ERK2 phosphorylation, DeltaFosB expression, and conditioned place preference to amphetamine and cocaine. *FASEB J.* 25, 2071–2081. doi: 10.1096/fj.10-175737

Marazziti, D., Gallo, A., Golini, E., Matteoni, R., and Tocchini-Valentini, G. P. (1998). Molecular cloning and chromosomal localization of the mouse Gpr37 gene encoding an orphan G-protein-coupled peptide receptor expressed in brain and testis. *Genomics* 53, 315–324. doi: 10.1006/geno.1998.5433

Marazziti, D., Golini, E., Mandillo, S., Magrelli, A., Witke, W., Matteoni, R., et al. (2004). Altered dopamine signaling and MPTP resistance in mice lacking the Parkinson's disease-associated GPR37/parkin-associated endothelin-like receptor. *Proc. Natl. Acad. Sci. U.S.A.* 101, 10189–10194. doi: 10.1073/pnas.0403661101

Moore, G. J., Bebchuk, J. M., Parrish, J. K., Faulk, M. W., Arfken, C. L., Strahl-Bevacqua, J., et al. (1999). Temporal dissociation between lithium-induced changes in frontal lobe myo-inositol and clinical response in manic-depressive illness. *Am. J. Psychiatry* 156, 1902–1908.

Neal, Jr. C. R., Akil, H., and Watson, Jr. S. J. (2001). Expression of orphanin FQ and the opioid receptor-like (ORL1) receptor in the developing human and rat brain. *J. Chem. Neuroanat.* 22, 219–249. doi: 10.1016/S0891-0618(01)00135-1

Pachter, J. A., Pai, J. K., Mayer-Ezell, R., Petrin, J. M., Dobek, E., and Bishop, W. R. (1992). Differential regulation of phosphoinositide and phosphatidylcholine hydrolysis by protein kinase C-beta 1 overexpression. Effects on stimulation by alpha-thrombin, guanosine 5'-O-(thiotriphosphate), and calcium. *J. Biol. Chem.* 267, 9826–9830.

Pandey, G. N., Dwivedi, Y., Pandey, S. C., Conley, R. R., Roberts, R. C., and Tamminga, C. A. (1997). Protein kinase C in the postmortem brain of teenage suicide victims. *Neurosci. Lett.* 228, 111–114. doi: 10.1016/S0304-3940(97)00378-9

Pandey, G. N., Dwivedi, Y., Rizavi, H. S., Ren, X., Pandey, S. C., Pesold, C., et al. (2002). Higher expression of serotonin 5-HT(2A) receptors in the postmortem brains of teenage suicide victims. *Am. J. Psychiatry* 159, 419–429. doi: 10.1176/appi.ajp.159.3.419

Peeters, P. J., Fierens, F. L., van den Wyngaert, I., Goehlmann, H. W., Swagemakers, S. M., Kass, S. U., et al. (2004). Gene expression profiles highlight adaptive brain mechanisms in corticotropin releasing factor overexpressing mice. *Brain Res. Mol. Brain Res.* 129, 135–150. doi: 10.1016/j.molbrainres.2004.06.038

Quintero, J. L., Arenas, M. I., and Garcia, D. E. (2005). The antidepressant imipramine inhibits M current by activating a phosphatidylinositol 4, 5-bisphosphate (PIP(2))-dependent pathway in rat sympathetic neurones. *Br. J. Pharmacol.* 145, 837–843. doi: 10.1038/sj.bjp.0706239

Racagni, G., and Popoli, M. (2008). Cellular and molecular mechanisms in the long-term action of antidepressants. *Dialogues Clin. Neurosci.* 10, 385–400.

Robbins, M. J., Charles, K. J., Harrison, D. C., and Pangalos, M. N. (2002). Localisation of the GPRC5B receptor in the rat brain and spinal cord. *Brain Res. Mol. Brain Res.* 106, 136–144. doi: 10.1016/S0169-328X(02)00420-5

Rogers, M. A., Kasai, K., Koji, M., Fukuda, R., Iwanami, A., Nakagome, K., et al. (2004). Executive and prefrontal dysfunction in unipolar depression: a review of neuropsychological and imaging evidence. *Neurosci. Res.* 50, 1–11. doi: 10.1016/j.neures.2004.05.003

Ruhe, H. G., Mason, N. S., and Schene, A. H. (2007). Mood is indirectly related to serotonin, norepinephrine and dopamine levels in humans: a meta-analysis of monoamine depletion studies. *Mol. Psychiatry* 12, 331–359. doi: 10.1038/sj.mp.4001949

Sano, T., Kim, Y. J., Oshima, E., Shimizu, C., Kiyonari, H., Abe, T., et al. (2011). Comparative characterization of GPRC5B and GPRC5CLacZ knockin mice; behavioral abnormalities in GPRC5B-deficient mice. *Biochem. Biophys. Res. Commun.* 412, 460–465. doi: 10.1016/j.bbrc.2011.07.118

Serretti, A. (2002). Lithium long-term treatment in mood disorders: clinical and genetic predictors. *Pharmacogenomics* 3, 117–129. doi: 10.1517/14622416.3.1.117

Sherrin, T., Heng, K. Y., Zhu, Y. Z., Tang, Y. M., Lau, G., and Tan, C. H. (2004). Cholecystokinin-B receptor gene expression in cerebellum, pre-frontal cortex and cingulate gyrus and its association with suicide. *Neurosci. Lett.* 357, 107–110. doi: 10.1016/j.neulet.2003.11.072

Sibille, E., Arango, V., Galfalvy, H. C., Pavlidis, P., Erraji-Benchekroun, L., Ellis, S. P., et al. (2004).Gene expression profiling of depression and suicide in human prefrontal cortex. *Neuropsychopharmacology* 29, 351–361. doi: 10.1038/sj.npp.1300335

Sinha, D., Wang, Z., Ruchalski, K. L., Levine, J. S., Krishnan, S., Lieberthal, W., et al. (2005). Lithium activates the Wnt and phosphatidylinositol 3-kinase Akt signaling pathways to promote cell survival in the absence of soluble survival factors. *Am. J. Physiol. Renal Physiol.* 288, F703–F713. doi: 10.1152/ajprenal.00189.2004

Spleiss, O., van Calker, D., Scharer, L., Adamovic, K., Berger, M., and Gebicke-Haerter, P. J. (1998). Abnormal G protein alpha(s) - and alpha(i2)-subunit mRNA expression in bipolar affective disorder. *Mol. Psychiatry* 3, 512–520. doi: 10.1038/sj.mp.4000393

Steen, V. M., Lovlie, R., Osher, Y., Belmaker, R. H., Berle, J. O., and Gulbrandsen, A. K. (1998). The polymorphic inositol polyphosphate 1-phosphatase gene as a candidate for pharmacogenetic prediction of lithium-responsive manic-depressive illness. *Pharmacogenetics* 8, 259–268.

Storey, J. D., and Tibshirani, R. (2003). Statistical significance for genomewide studies. *Proc. Natl. Acad. Sci. U.S.A.* 100, 9440–9445. doi: 10.1073/pnas.1530509100

Takuwa, Y., Takuwa, N., and Sugimoto, N. (2002). The Edg family G protein-coupled receptors for lysophospholipids: their signaling properties and biological activities. *J. Biochem.* 131, 767–771. doi: 10.1093/oxfordjournals.jbchem.a003163

Tomita, H., Vawter, M. P., Walsh, D. M., Evans, S. J., Choudary, P. V., Li, J., et al. (2004). Effect of agonal and postmortem factors on gene expression profile: quality control in microarray analyses of postmortem human brain. *Biol. Psychiatry* 55, 348–354. doi: 10.1016/j.biopsych.2003.10.013

Vawter, M. P., Tomita, H., Meng, F., Bolstad, B., Li, J., Evans, S., et al. (2006). Mitochondrial-related gene expression changes are sensitive to agonal-pH state: implications for brain disorders. *Mol. Psychiatry* 11, 615, 663–679. doi: 10.1038/sj.mp.4001830

Wise, A., Jupe, S. C., and Rees, S. (2004). The identification of ligands at orphan G-protein coupled receptors. *Annu. Rev. Pharmacol. Toxicol.* 44, 43–66. doi: 10.1146/annurev.pharmtox.44.101802.121419

Xu, X., Muller-Taubenberger, A., Adley, K. E., Pawolleck, N., Lee, V. W., Wiedemann, C., et al. (2007). Attenuation of phospholipid signaling provides a novel mechanism for the action of valproic acid. *Eukaryot Cell* 6, 899–906. doi: 10.1128/EC.00104-06

Young, L. T., Asghari, V., Li, P. P., Kish, S. J., Fahnestock, M., and Warsh, J. J. (1996). Stimulatory G-protein alpha-subunit mRNA levels are not increased in autopsied cerebral cortex from patients with bipolar disorder. *Brain Res. Mol. Brain Res.* 42, 45–50. doi: 10.1016/S0169-328X(96)00112-X

Young, L. T., Li, P. P., Siu, K. P., Kish, S. J., and Warsh, J. J. (1993). Regional distribution of guanine nucleotide binding proteins (Gs and Gi alpha) in human brain: correlation with adenylyl cyclase activity. *Neurochem. Int.* 22, 285–291. doi: 10.1016/0197-0186(93)90057-C

Zeng, Z., Su, K., Kyaw, H., and Li, Y. (1997). A novel endothelin receptor type-B-like gene enriched in the brain. *Biochem. Biophys. Res. Commun.* 233, 559–567. doi: 10.1006/bbrc.1997.6408

Zhou, J. N., Riemersma, R. F., Unmehopa, U. A., Hoogendijk, W. J., van Heerikhuize, J. J., Hofman, M. A., et al. (2001). Alterations in arginine vasopressin neurons in the suprachiasmatic nucleus in depression. *Arch. Gen. Psychiatry* 58, 655–662. doi: 10.1001/archpsyc.58.7.655

Conflict of Interest Statement: The authors declare that the research was conducted in the absence of any commercial or financial relationships that could be construed as a potential conflict of interest.

Received: 26 February 2013; accepted: 05 December 2013; published online: 23 December 2013.

Citation: Tomita H, Ziegler ME, Kim HB, Evans SJ, Choudary PV, Li JZ, Meng F, Dai M, Myers RM, Neal CR, Speed TP, Barchas JD, Schatzberg AF, Watson SJ, Akil H, Jones EG, Bunney WE and Vawter MP (2013) G protein-linked signaling pathways in bipolar and major depressive disorders. Front. Genet. 4:297. doi: 10.3389/fgene.2013.00297

This article was submitted to Behavioral and Psychiatric Genetics, a section of the journal Frontiers in Genetics.

PLOS ONE

Association of *HK2* and *NCK2* with Normal Tension Glaucoma in the Japanese Population

Dong Shi[1,2], Tomoyo Funayama[3], Yukihiko Mashima[4], Yoshimasa Takano[1], Ai Shimizu[1], Kotaro Yamamoto[1], MinGe Mengkegale[1], Akiko Miyazawa[1], Noriko Yasuda[5], Takeo Fukuchi[6], Haruki Abe[6], Hidenao Ideta[7], Kohji Nishida[8], Toru Nakazawa[1], Julia E. Richards[9,10], Nobuo Fuse[1,11]*

1 Department of Ophthalmology, Tohoku University Graduate School of Medicine, Sendai, Miyagi, Japan, **2** Department of Ophthalmology, the Fourth Affiliated Hospital, China Medical University, Shenyang, Liaoning, China, **3** Department of Chemistry, Faculty of Education, Bunkyo University, Koshigaya, Saitama, Japan, **4** Department of Ophthalmology, Keio University School of Medicine, Shinjuku-ku, Tokyo, Japan, **5** Department of Ophthalmology, Tokyo Metropolitan Police Hospital, Tokyo, Japan, **6** Division of Ophthalmology and Visual Science, Graduate School of Medical and Dental Sciences, Niigata University, Niigata, Japan, **7** Ideta Eye Hospital, Kumamoto, Japan, **8** Department of Ophthalmology, Osaka University Graduate School of Medicine, Suita, Osaka, Japan, **9** Department of Ophthalmology and Visual Sciences, W. K. Kellogg Eye Center, University of Michigan, Ann Arbor, Michigan, United States of America, **10** Department of Epidemiology, University of Michigan, Ann Arbor, Michigan, United States of America, **11** Department of Integrative Genomics, Tohoku Medical Megabank Organization, Sendai, Miyagi, Japan

Abstract

Although family studies and genome-wide association studies have shown that genetic factors play a role in glaucoma, it has been difficult to identify the specific genetic variants involved. We tested 669 single nucleotide polymorphisms (SNPs) from the region of chromosome 2 that includes the GLC1B glaucoma locus for association with primary open-angle glaucoma (POAG) and normal tension glaucoma (NTG) in the Japanese population. We performed a two-stage case-control study. The first cohort consisted of 123 POAG cases, 121 NTG cases and 120 controls: the second cohort consisted of 187 POAG cases, 286 NTG cases, and 271 controls. Out of six SNPs showing significant association with POAG in the first round screening, seven SNPs were tested in the second round. Rs678350 in the *HK2* gene coding sequence showed significant allelic ($p = 0.0027$ in Stage Two, 2.7XE-4 in meta-analysis) association with POAG, and significant allelic ($p = 4.7$XE-4 in Stage Two, 1.0XE-5 in meta-analysis) association with NTG. Although alleles in the *TMEM182* gene did not show significant association with glaucoma in the second round, subjects with the A/A allele in *TMEM182* rs869833 showed worse visual field mean deviation ($p = 0.01$). Even though rs2033008 in the *NCK2* gene coding sequence did not show significant association in the first round, it had previously shown association with NTG so it was tested for association with NTG in round 2 ($p = 0.0053$ in Stage Two). Immunohistochemistry showed that both *HK2* and *NCK2* are expressed in the retinal ganglion cell layer. Once multi-testing was taken into account, only *HK2* showed significant association with POAG and NTG in Stage Two. Our data also support previous reports of *NCK2* association with NTG, and raise questions about what role *TMEM182* might play in phenotypic variability. Our data suggest that *HK2* may play an important role in NTG in the Japanese population.

Citation: Shi D, Funayama T, Mashima Y, Takano Y, Shimizu A, et al. (2013) Association of *HK2* and *NCK2* with Normal Tension Glaucoma in the Japanese Population. PLoS ONE 8(1): e54115. doi:10.1371/journal.pone.0054115

Editor: Rajiv R. Mohan, University of Missouri-Columbia, United States of America

Received August 16, 2012; **Accepted** December 6, 2012; **Published** January 22, 2013

Funding: This study was supported in part by a Grant-In-Aid for Scientific Research from the Ministry of Education, Science, and Culture of the Japanese Government (C-22591928), Tokyo, Japan (NF); by a grant from the Ministry of Health, Labor and Welfare of Japan (NF); by Tohoku Medical Megabank Project (NF); by a grant from the Japan-China Medical Association (DS); by a grant R01-EY011671 from the National Eye Institute at the National Institutes of Health (JER), Bethesda, MD, USA; and a grant from Research to Prevent Blindness, New York, NY, USA (JER). The funders had no role in study design, data collection and analysis, decision to publish, or preparation of the manuscript.

Competing Interests: The authors have declared that no competing interests exist.

* E-mail: fusen@oph.med.tohoku.ac.jp

Introduction

Glaucoma is a complex, heterogeneous disease characterized by a progressive degeneration of the optic nerve fibers, and is the second highest cause of blindness worldwide affecting approximately 70 million people [1]. The most common type of open-angle glaucoma, primary open-angle glaucoma (POAG), is associated with elevated intraocular pressure (IOP) [2], and another less-common subgroup of open-angle glaucoma, called low-tension glaucoma (LTG) [3,4] or normal tension glaucoma (NTG) is associated with IOP that does not rise outside of the normal range [5]. The prevalence of NTG is reported to be higher among the Japanese than among Caucasians [6,7]. This is an important medical and public health problem because simple screening programs based on detection of elevated IOP are not effective in a population where NTG is highly prevalent. Thus, an accurate diagnostic test for presymptomatic detection of individuals at risk for glaucoma, especially NTG in Japan, is urgently needed.

Open-angle glaucoma is a genetically heterogeneous disorder attributed to the interaction of multiple genes and environmental factors [8,9]. More than 15 POAG loci have been identified by linkage, and five open-angle glaucoma genes located within those loci have been identified [10,11]. More recently, genome-wide association studies (GWAS) using high-density single nucleotide polymorphism (SNP) arrays have been used to identify genetic risk factors involved in the common, complex forms of open-angle glaucoma that do not show classical Mendelian inheritance

patterns. Burdon et al. identified susceptibility loci at TMCO1 and CDKN2B-AS1 that contribute to severe forms of glaucoma [12]. Ramdas et al. used meta-analysis of data from six separate studies to find significant evidence that three common variants of CDKN2B, ATOH7 and SIX1 are associated with POAG [13]. Wiggs et al. found significant evidence that genetic variants in CDKN2B-AS1 and a gene desert on 8q22 are associated with optic nerve damage in glaucoma [14].

Based on a linkage study involving 6 Caucasian families in the UK, the *GLC1B* locus for adult-onset open-angle glaucoma was identified at chromosome 2cen–q13 [15]. The patients in these families had clinical characteristics of low to moderate IOP, disease onset in their late 40 s, and a good response to medical therapy, and those phenotypes mimic the majority of Japanese NTG cases. Thus, the screening of the gene around GLC1B locus may be useful for diagnosis of POAG and NTG in the general Japanese population.

The purpose of this study was to screen for candidate genes for POAG and NTG on chromosome 2, around the GLC1B (glaucoma 1, open angle, B) locus in unrelated Japanese patients, using high density SNP scanning and case-control association. Here we report one gene that shows significant association with POAG and NTG, support for a previously reported association with NTG, and a gene for which genotype is predictive of severity of mean deviation on the visual field test.

Results

A Two-stage Case-control Study of SNPs on Chromosome2

To identify a gene associated with glaucoma we did a high-density scan of the region around GLC1B on chromosome 2 by screening 669 SNPs on chromosome 2 in a two-stage case-control study design (Figure 1). We were especially interested in whether any SNPs that fall within genes in the GLC1B region might be associated with POAG or NTG (Table 1). Among genes from this region we found fourteen SNPs that show significant evidence of association with POAG, and nine SNPs that show significant evidence of association with NTG. Four of the SNP alleles which show significant evidence of association are identical between the POAG and NTG subjects.

We identified six SNPs in Stage One that showed evidence of association with POAG (rs1239066, rs1529385, rs869833, rs960011, rs1027003) and two SNPs (rs678350, rs2033008) that showed association with NTG (Figure 2 and Table 2). The SNPs rs869833 and rs960011 are located within the *TMEM182* gene, which contains 5 exons and 229 amino acids. The amino acid sequence of *TMEM182* predicts an evolutionarily-conserved novel transmembrane protein, which consists of four putative membrane-spanning regions indicative of an integral membrane topology. The SNP rs678350 is located within the *Hexokinase 2 (HK2)* gene which contains 18 exons and 917 amino acids. The SNP rs678350 exists on intron1 of *HK2* gene. The *HK2* gene produces a protein product localizes on the outer membrane of mitochondria and plays an important role in intracellular glucose metabolism by catalyzing the conversion of glucose to glucose-6-phosphate. There are no known genes closely neighboring the SNP rs1239066 and rs1027003. We have checked the SNPs near rs1529385 within LOC129293 and TMSB10 and did not find get any positive polymorphisms.

We selected three genes for second stage mutation screening. *TMEM182* and *HK2* genes were selected because they contain SNPs that showed significant evidence of association in Stage One in this study. Even though SNPs in the *NCK2* gene showed significant evidence of association (p = 0.014), the *NCK2* gene was selected for second stage mutation screening based of the previous report that it is associated with NTG [16].

The SNP rs1239066 showed significant evidence of association in both Stage One and Stage Two screenings. In the meta-analysis it showed significant evidence of association (POAG, NTG; P = 0.001, 0.005), as did rs1027003 (POAG; P = 0,010) (Table 2).

HK2 Variants Detected in this Study

The SNP rs678350 in the *HK2* gene coding sequence showed significant allelic (p = 0.0027 in Stage Two, 2.7XE-4 in meta-analysis) association with POAG, and significant allelic (p = 4.7XE-4 in Stage Two, 1.0XE-5 in meta-analysis) association

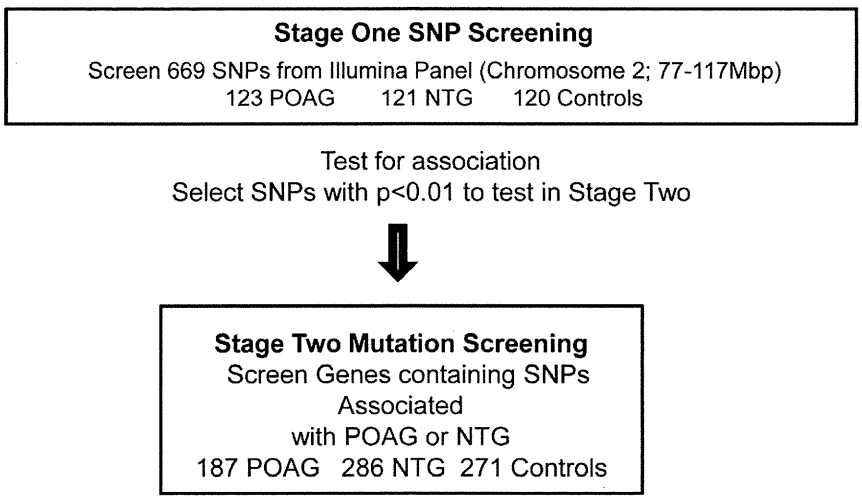

Figure 1. Experimental Study Design. The study used a first stage of SNP screening in one population to identify SNPs and genes to be tested in a second population through SNP association testing and mutation screening of genes containing SNPs associated with glaucoma. Stage Two tested SNPs for association in a second population and did mutation screening in that second population in genes containing SNPs that showed significant association with POAG or NTG ($p<0.01$) in Stage One of our study or that had been previously reported to show significant evidence of association [16].
doi:10.1371/journal.pone.0054115.g001

Table 1. Stage one Test of SNPs in GLC1B-Region Genes for Association with POAG or NTG.

Genomic Information			POAG			NTG			Control
rs number	Location	Gene Symbol	MAF	Odds ratio (CI)	p value*	MAF	Odds ratio (CI)	p value*	MAF
rs741788	2p13	*DCTN1*	0.455	1.47 (1.02–2.12)	0.038	0.455	1.47 (1.02–2.11)	0.040	0.363
rs909177		*DCTN1*	0.455	1.44 (1.00–2.08)	0.047	0.463	1.49 (1.03–2.14)	0.032	0.367
rs740277		*DCTN1*	0.455	1.44 (1.00–2.08)	0.047	0.463	1.49 (1.03–2.14)	0.032	0.367
rs678350	2p13	*HK2*	0.333	1.50 (1.01–2.23)	0.043	0.371	1.77 (1.19–2.62)	0.004	0.250
rs651071		*HK2*	0.199	0.60 (0.40–0.92)	0.018	0.256	0.84 (0.56–1.25)	0.383	0.292
rs1807090		*HK2*	0.268	1.59 (1.03–2.44)	0.034	0.238	1.35 (0.87–2.10)	0.181	0.188
rs1239066	2p12		0.293	3.04 (1.95–4.72)	0.009	0.269	1.55 (1.01–2.38)	0.045	0.192
rs53915	2p12-p11.1	*CTNNA2*	0.199	0.64 (0.42–0.98)	0.039	0.260	0.91 (0.61–1.36)	0.641	0.279
rs1529385	2p11.2	*LOC129293 (C2orf89)*	0.053	0.39 (0.20–0.77)	0.005	0.087	0.66 (0.37–1.20)	0.173	0.125
rs1053561	2p11.2	*TGOLN2*	0.114	0.53 (0.32–0.88)	0.012	0.178	0.89 (0.56–1.40)	0.609	0.196
rs1562322	2p11.2	*LOC51255 (RNF181)*	0.321	0.88 (0.61–1.29)	0.520	0.256	0.64 (0.43–0.95)	0.027	0.349
rs3024831	2p12-p11.2	*SFTPB*	0.250	0.92 (0.61–1.38)	0.675	0.190	0.65 (0.42–0.99)	0.045	0.267
rs6875	2q11.2	*RW1 (TMEM131)*	0.008	0.21 (0.05–0.98)	0.030	0.025	0.66 (0.23–1.88)	0.431	0.038
rs1982336		*RW1 (TMEM131)*	0.008	0.23 (0.05–1.05)	0.027	0.029	0.75 (0.28–2.05)	0.576	0.038
rs718159		*RW1 (TMEM131)*	0.008	0.21 (0.05–0.98)	0.028	0.029	0.76 (0.28–2.07)	0.587	0.038
rs222	2q11.2	*INPP4A*	0.183	0.69 (0.44–1.06)	0.091	0.161	0.59 (0.38–0.93)	0.021	0.246
rs1530028	2q11.2	*FLJ45273 (LONRF2)*	0.228	0.66 (0.44–0.99)	0.045	0.306	0.99 (0.67–1.46)	0.952	0.308
rs1030902	2q11.2	*ALS2*	0.225	0.65 (0.44–0.98)	0.039	0.314	1.03 (0.70–1.51)	0.892	0.308
rs1369482	2q11.2	*NPAS2*	0.244	0.65 (0.43–0.96)	0.030	0.298	0.85 (0.58–1.24)	0.398	0.333
rs871656	2q12	*IL1R1*	0.337	0.70 (0.49–1.01)	0.058	0.322	0.66 (0.45–0.95)	0.025	0.421
rs878539	2q11.2	*SLC9A2 (NHE2)*	0.463	1.52 (1.06–2.18)	0.024	0.422	1.28 (0.89–1.85)	0.185	0.363
rs869833	2q12.1	*TMEM182*	0.467	1.66 (1.15–2.40)	0.006	0.376	1.14 (0.79–1.65)	0.490	0.346
rs960011		*TMEM182*	0.415	0.57 (0.40–0.82)	0.001	0.512	0.85 (0.60–1.21)	0.232	0.554**
rs2033008	2q12	*NCK2*	0.293	0.76 (0.51–1.11)	0.147	0.252	0.62 (0.42–0.91)	0.015	0.354
rs1027003	2q12		0.110	3.16 (1.46–6.88)	0.002	0.058	1.58 (0.67–3.71)	0.295	0.038
rs1474220	2q12.3	*GCC2*	0.106	0.59 (0.35–1.00)	0.050	0.136	0.79 (0.48–1.30)	0.353	0.167
rs899259	2q13	*EDAR*	0.098	0.66 (0.38–1.14)	0.134	0.075	0.49 (0.28–0.90)	0.019	0.142
rs1509414	2q13	*BENE(MALL)*	0.037	0.40 (0.18–0.88)	0.020	0.041	0.45 (0.21–0.98)	0.039	0.096
rs1567366	2q13	*NPHP1*	0.561***	1.34 (0.94–1.92)	0.105	0.576***	1.44 (1.01–2.07)	0.045	0.488
rs2119112	2q14.2	*MARCO*	0.110	0.57 (0.34–0.95)	0.029	0.107	0.55 (0.33–0.93)	0.025	0.179

*chi-square test.
**minor allele frequency in stage 2 control was 0.494.
***minor allele in control was major allele in POAG and NTG subjects.
MAF; minor allele frequency, CI; confidence interval.
doi:10.1371/journal.pone.0054115.t001

with NTG (Table 2). The rs678350 showed also a significant difference in genotype frequency (p = 0.0046 and 0.0039) in the POAG and NTG groups (Table 3). In the second round, we screened the *HK2* coding sequence and intron-exon boundaries for mutations in POAG and NTG patients. After direct sequencing, we found 2 coding SNPs; p.Gln142His (A/T at the third nucleotide; rs2229621) in exon 4 and p.Arg844Lys (G/A at the second nucleotide; rs2229629) in exon 17. The allelic frequency of the p.Gln142His (A/T) variant was significantly higher in the NTG group than in the control group (p = 0.025), but it was not higher in the POAG group than in the control group (p = 0.181). The genotype frequency of the p.Gln142His (A/T) variant (dominant model) was significantly higher in the NTG group than in the control group (p = 0.019) but we did not find evidence that the frequency in the POAG group was different from the control group (p = 0.179). There was no evidence of a significant difference between POAG and NTG for p.Arg844Lys. No other mutation was found. We tested the LD block and found no linkage disequilibrium between SNPs rs678350 and rs2229621 (D′ = 0.08). We tested the correlation between the phenotypes POAG or NTG and the genotypes screened in the second stage screening of HK2, and found no association with any phenotypes including age at diagnosis, maximum IOP under medication, and MD value of the visual field (Table 4). None of the polymorphisms showed deviation from Hardy–Weinberg equilibrium ($P<0.05$).

NCK2 Variants Detected in this Study

The SNP rs2033008 in the *NCK2* gene showed a significant difference in allelic frequency (p = 0.015 in Stage One, p = 0.0053 in Stage Two, and 2.2XE-4 in meta-analysis) between controls and NTG, but not between control and POAG status (p = 0.147 in Stage One, 0.35 in Stage Two, 0.12 in meta-analysis) (Table 2 and

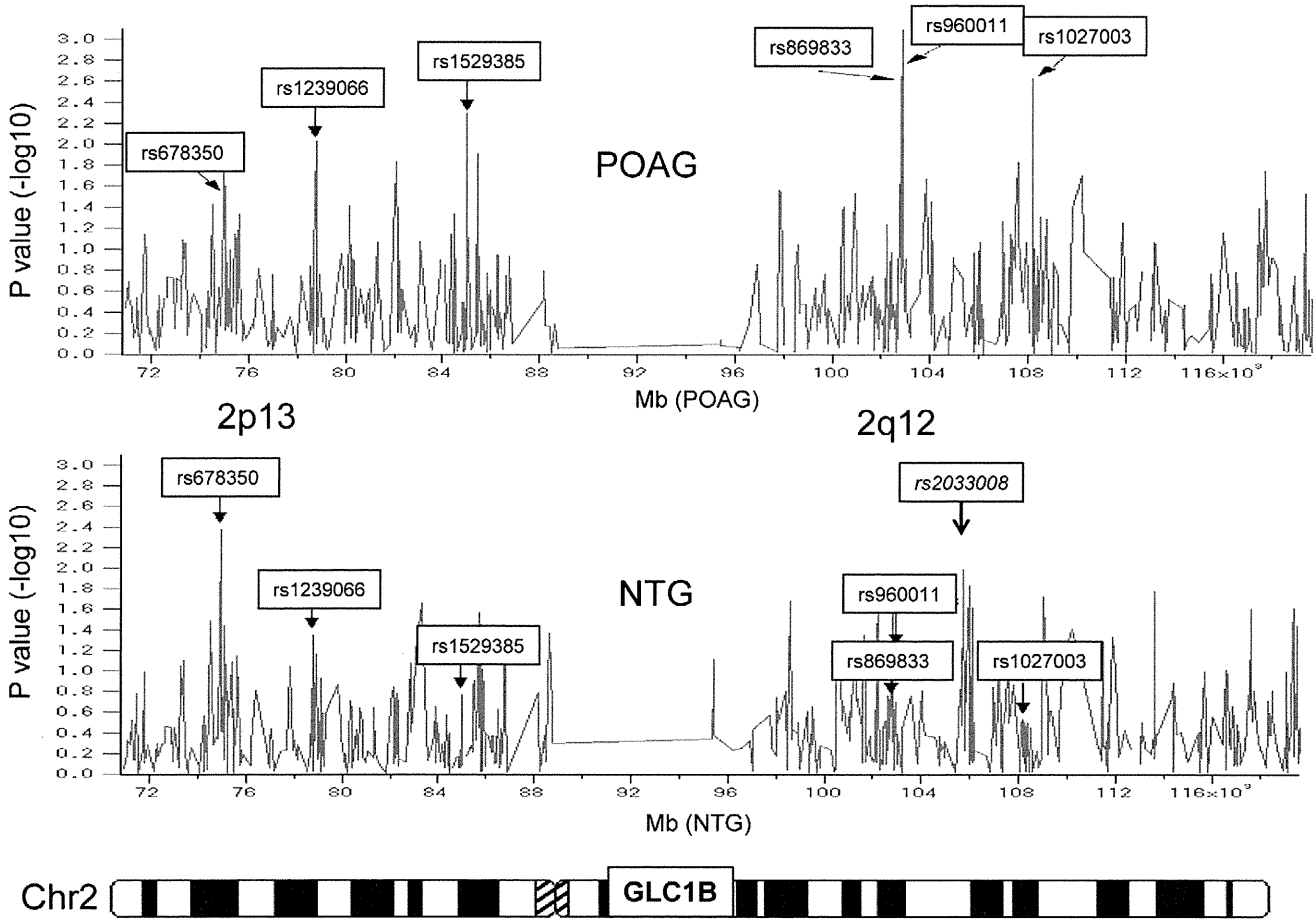

Figure 2. High-density scan of the GLC1B region on chromosome 2 to identify candidate glaucoma genes. Six SNPs that showed significant evidence of association with POAG or NTG ($p<0.01$) and the previously-reported candidate *NCK2* gene are shown. Vertical line shows p value (−log10), and horizontal line shows chromosomal location (kb).
doi:10.1371/journal.pone.0054115.g002

Table 5). The odds ratio for association with NTG supports a model in which *NCK2* is associated with NTG; OR = 0.69 (0.53–0.89), but the odds ratio for association with POAG was not significant; 0.87 (0.65–1.16) in Stage Two. Only this rs2033008 polymorphism in Stage One showed deviation from Hardy–Weinberg equilibrium ($p = 0.030$).

We screened the sequence of the *NCK2* coding sequence and intron-exon boundaries for mutations in POAG and NTG patients and found 1 synonymous coding base change: Thr14Thr (ACC >ACT) in one NTG subject. Although SNP rs2033008 showed significant association but the Thr14Thr variant showed no statistical difference in allele frequency between NTG and normal subjects ($p = 0.33$). The Thr14Thr heterozygotes (A/A) in the NTG subjects have the worse Mean Deviation value of the visual field compared with human reference sequence (T/T) ($p = 0.05$) (Table 6).

The single NTG subject with the Thr14Thr variant was a 50 year old woman whose father also had NTG. Her age at diagnosis was 40 years old. Her initial IOP was 15 mmHg in each eye. The mean deviation (MD) of the visual field test was −3.87 dB in the right eye, and −1.97 dB in the left eye, reflecting a mild NTG phenotype.

TMEM182 Variants Detected in this Study

We found no mutations in *TMEM182* coding sequence and intron-exon boundaries, for mutations in POAG and NTG patients. After finding association for SNPs rs869833 and rs960011 in the POAG and NTG subjects in Stage One, we did not find this association confirmed in Stage Two SNP testing (Table 7). When we tested for correlation between Stage Two case endophenotypes and TMEM182 genotype, we found association with the MD value of the visual field in POAG subjects. The POAG subjects homozygous for the A/A allele of SNP rs869833 have worse Mean Deviation value of the visual field test compared with those who carry the G/G genotype in Stage Two subjects ($p = 0.01$) (Table 8).

Immunohistochemistory of the *HK2* and *NCK2*

Representative immunohistochemistory (IHC) photographs with *Hk2, Nck2*, astrocyte marker (GFAP) and retinal ganglion cell marker (C38) on the retinas of untreated mice were shown (Fig. 3, A, B). *Hk2* and *Nck2* were strongly immunoreactive in the ganglion cell layer. C38 signals co-localized with *Hk2* or *Nck2* in the ganglion cell layer, as indicated by arrows (Fig. 3 A, B). *Hk2* expression is only located in the ganglion cell layer. *Nck* is expressed in the ganglion cell layer, inner nuclear layer, and outer plexiform layer, with the highest level of expression in the ganglion cell layer.

Discussion

HK2 in POAG and NTG subjects

The rs678350 in the *HK2* gene coding sequence showed significant allelic ($p = 0.043$ in Stage One, $p = 0.0027$ in Stage

Table 2. Stage One and Stage Two Association Test Results.

Stage One Screening

		POAG			NTG			CNTL
SNP	Minor Allele	MAF	Odds ratio	p value*	MAF	Odds ratio	p value*	MAF
rs1239066	C	0.293	3.04 (1.95–4.72)	0.009	0.269	1.55 (1.01–2.38)	0.045	0.192
rs1529385	T	0.053	0.39 (0.20–0.77)	0.005	0.087	0.66 (0.37–1.20)	0.173	0.125
rs869833	G	0.467	1.66 (1.15–2.40)	0.006	0.376	1.14 (0.79–1.65)	0.490	0.346
rs960011	T	0.415	0.57 (0.40–0.82)	0.001	0.512	0.85 (0.60–1.21)	0.232	0.554
rs1027003	G	0.110	3.16 (1.46–6.88)	0.002	0.058	1.58 (0.67–3.71)	0.295	0.038
rs678350	G	0.333	1.50 (1.01–2.23)	0.043	0.371	1.77 (1.19–2.62)	0.004	0.250
rs2033008	A	0.293	0.76 (0.51–1.11)	0.147	0.252	0.62 (0.42–0.91)	0.015	0.354

Stage Two Screening

		POAG			NTG			CNTL
SNP	Minor Allele	MAF	Odds ratio	p value*	MAF	Odds ratio	p value*	MAF
rs1239066	C	0.246	1.70 (1.09–2.65)	0.019	0.240	1.64 (1.06–2.51)	0.024	0.161
rs1529385	T	0.122	1.42 (0.73–2.77)	0.305	0.072	0.79 (0.37–1.68)	0.543	0.089
rs869833	G	0.409	0.98 (0.75–1.28)	0.855	0.421	1.03 (0.81–1.30)	0.834	0.415
rs960011	T	0.497	1.13 (0.86–1.47)	0.363	0.481	1.06 (0.84–1.34)	0.641	0.467
rs1027003	G	0.049	1.10 (0.42–2.90)	0.840	0.047	1.04 (0.30–2.83)	0.944	0.045
rs678350	G	0.334	1.58 (1.18–2.11)	0.0027	0.337	1.60 (1.23–2.08)	4.7XE-4	0.242
rs2033008	A	0.297	0.87 (0.65–1.16)	0.348	0.250	0.69 (0.53–0.89)	0.0053	0.327

Meta-analysis

		POAG			NTG			CNTL
SNP	Minor Allele	MAF	Odds ratio	p value*	MAF	Odds ratio	p value*	MAF
rs1239066	C	0.264	1.65 (1.22–2.23)	0.001	0.248	1.52 (1.14–2.04)	0.005	0.178
rs1529385	T	0.082	0.73 (0.46–1.16)	0.20	0.081	0.71 (0.45–1.14)	0.16	0.109
rs869833	G	0.432	1.17 (0.95–1.45)	0.16	0.408	1.06 (0.87–1.30)	0.54	0.393
rs960011	T	0.465	0.89 (0.72–1.10)	0.28	0.490	0.99 (0.81–1.20)	0.92	0.494
rs1027003	G	0.084	2.17 (1.20–3.92)	0.010	0.053	1.32 (0.69–2.53)	0.42	0.041
rs678350	G	0.334	1.56 (1.23–1.96)	2.7XE-4	0.347	1.65 (1.32–2.05)	1.0XE-5	0.244
rs2033008	A	0.295	0.83 (0.66–1.04)	0.12	0.251	0.66 (0.53–0.82)	2.2XE-4	0.335

MAF; Minor allele frequency, CNTL; Control.
*Fisher's exact test.
doi:10.1371/journal.pone.0054115.t002

Table 3. Stage Two *HK2* SNPs Allele Frequencies in Japanese POAG, NTG and Control Subjects.

	Allele frequency				Genotype			
rs678350	**A**	**G**	**Odds ratio (CI)**	**p value***	**A/A**	**A/G**	**G/G**	**p value***
POAG	0.666	0.334	1.58 (1.18–2.11)	0.0027	82/187	85/187	20/187	0.0046
NTG	0.663	0.337	1.60 (1.23–2.08)	4.7XE-4	133/286	113/286	40/286	0.0039
Control	0.758	0.242			161/271	89/271	21/271	
	Allele frequency				**Genotype**			
rs2229621/Q142H	**A**	**T**	**Odds ratio (CI)**	**p value***	**A/A**	**A/T**	**T/T**	**p value***
POAG	0.738	0.262	1.24 (0.92–1.69)	0.181	102/187	72/187	13/187	0.179
NTG	0.719	0.281	1.36 (1.04–1.79)	0.025	146/286	119/286	21/286	0.019
Control	0.777	0.223			165/271	91/271	15/271	

*Fisher's exact test; dominant model.
G/G or T/T is mutant homozygote, A/G or A/T is heterozygote, and A/A is wild homozygote.
doi:10.1371/journal.pone.0054115.t003

Two, 2.7XE-4 in meta-analysis association with POAG, and significant allelic (p = 0.004 in Stage One, p = 4.7XE-4 in Stage Two, 1.0XE-5 in meta-analysis) association with NTG (Table 2). The rs678350 polymorphism showed a significant case-control difference in genotype frequency ($p = 0.0046$ and 0.0039) in the POAG and NTG groups (Table 3). However, there was no association of this SNP with glaucoma endophenotypes including age at diagnosis, maximum intra ocular pressure under medication, and MD value of the visual field. So the *HK2* gene may contribute to disease susceptibility to POAG and NTG, but may not account for all of the phenotypic variability between individuals whose glaucoma results from variants in this gene. Our association findings suggest that the *HK2* gene that contains this polymorphism might play a role in POAG and NTG in the Japanese population, but it remains to be seen whether rs678350 is actually causative, perhaps through altering transcription or splicing, or whether another allele(s) in this gene or its regulatory region might actually be causing the disease. There remains a possibility that the p.Gln142His (A/T) SNP in *HK2* may play a role in disease pathology, but our study can only show association, not causation. Because none of our subjects come from the original families used to map the GLC1B locus, we can only draw conclusions regarding the possible role of this gene in the Japanese population, but this finding raises questions about whether this could be the GLC1B gene.

The HK2 gene product plays an important role in intracellular glucose metabolism by catalyzing the conversion of glucose to glucose-6-phosphate. The *HK2* gene localizes to the outer membrane of mitochondria. Since reduced glucose-6-phosphate content in muscle has been demonstrated in pre-non-insulin-dependent diabetes mellitus (pre-NIDDM) and NIDDM subjects, *HK2* was investigated as a promising candidate gene for noninsulin-dependent diabetes mellitus (NIDDM; OMIM125853) [17,18]; however, those studies concluded that mutations of the *HK2* gene, including a common p.Gln142His polymorphism is not a major etiologic factor for NIDDM in the Finnish [17,18,19,20], British [19], and Danish [20] populations. In brain, mitochondrial-hexokinase activity plays a key antioxidant role protecting against oxidative stress (ROS) [21], and complements the classical antioxidant enzymes that protect against oxidative stress [22]. Hexokinase antagonizes the release of mitochondrial cytochrome C activation of Akt, which is recognized as a potent inhibitor of apoptosis. *HK2* is probably associated with an anti-oxidative reaction and inhibition of apoptosis through Bax/Bak-mediated cytochrome *c* release [23]. Leber's hereditary optic neuropathy (LHON) -associated mitochondrial DNA mutations were found in Japanese patients with POAG [24], so it is reasonable to consider a gene whose product plays a role in mitochondria as a candidate gene for other phenotypes involving optic neuropathy.

NCK2 genes in POAG and NTG subjects

The *NCK2* gene, which was previously reported to be associated with NTG [16], encodes a member of the NCK family of adaptor proteins, and the adaptor protein which associates with tyrosine-phosphorylated growth factor receptors of their cellular substrates. SH2/SH3 domain-containing adapter proteins, such as the NCK family, play a major role in regulating tyrosine kinase signaling [25]. Previously, microsatellite marker D2S176 within the GLC1B locus showed significant association with NTG in the Japanese population, and D2S176 is located 24 kb from the *NCK2* gene [16]. Brain-derived neurotrophic factor (BDNF) binds to and activates the TrkB tyrosine kinase receptor to regulate cell differentiation and survival in the nervous system. BDNF

Table 4. Correlation between the POAG or NTG Endophenotypes and *HK2* SNPs Screened in Stage Two.

Endophenotype	Age at diagnosis (y.o.)				Maximum IOP* (mmHg)				MD value of the visual field (dB)			
rs678350 genotype	**A/A**	**A/G**	**G/G**	**p value****	**A/A**	**A/G**	**G/G**	**p value****	**A/A**	**A/G**	**G/G**	**p value****
POAG	61.6	55.3	59.0	0.83	24.0	23.6	21.9	0.56	−14.82	−15.64	−11.94	0.53
NTG	57.5	54.9	56.9	0.99	17.1	16.0	17.6	0.64	−10.72	−12.10	−7.14	0.37
rs2229621 genotype	**A/A**	**A/T**	**T/T**	**p value****	**A/A**	**A/T**	**T/T**	**p value****	**A/A**	**A/T**	**T/T**	**p value****
POAG	58.5	58.0	55.5	0.93	24.4	22.9	25.5	0.94	−16.42	−11.94	−17.65	0.65
NTG	57.8	55.2	57.4	0.91	16.1	17.5	16.9	0.63	−11.93	−10.34	−11.16	0.95

*IOP; intraocular pressure (under medication).
**Dunnett's test.
G/G or T/T is mutant homozygote, A/G or A/T is heterozygote, and A/A is wild homozygote.
doi:10.1371/journal.pone.0054115.t004

stimulation promotes interaction of *Nck2* with TrkB in cortical neuron [26]. And BDNF signaling in glia is known to play important roles in neural protection and regeneration, particularly in conversion of Muller glia to photoreceptors [27]. In our study, it is interesting that the *NCK2* variant rs2033008 showed a significantly difference from the control population in the NTG group, where the disease pathology seems to be focused on the retinal ganglion cells and the optic nerve, but not in the POAG group, where a substantial disease component localizes to the anterior chamber of the eye (Table 5). Thus although our study falls short of achieving a level of significance needed to identify *NCK2* de novo as a glaucoma gene and this polymorphism showed deviation from Hardy–Weinberg equilibrium ($p = 0.030$ in Stage One), our data do support the prior finding of significant allele frequency differences between NTG cases and normal controls in the Japanese population [16]. It is unclear whether this deviation from Hardy-Weinberg equilibrium in Stage One might represent the absence of some alleles from this population because they are associated with diagnoses specifically excluded from this study, such as ocular hypertension.

Immunohistochemistory of the *Hk2* and *Nck2*

Although KH2 and NCK2 had previously been detected in retina, more precise localization to specific cell types is needed to begin understanding how the gene products might play a role in disease pathology. In the representative IHC photographs, antibody against *Hk2* was strongly immunoreactive in the ganglion cell layer (GCL). The *Hk2* protein localizes to the outer membrane of mitochondria, and interestingly the *Hk2* protein appears in the GCL. *Nck2*, which interacts with BDNF, is expressed in ganglion cell layer (GCL), inner nuclear layer (INL) and outer plexiform layer (OPL), and most expressed in GCL. This localization makes it highly conceivable that the *Hk2 gene products* could each play a role in glaucoma, and there is possibility that *Nck2* could have relationship with glaucoma.

TMEM182 in POAG and NTG

SNPs rs869833 and rs960011 in the TMEM182 gene showed significant association with POAG and NTG in Stage One that was not confirmed in the second stage. The primary amino acid sequence of *TMEM182* predicts an evolutionarily-conserved novel transmembrane protein, which consists of four putative membrane-spanning regions indicative of an integral membrane topology. The *TMEM182* protein sequence lacks homologies with previously-defined protein families. However, the pro-inflammatory cytokine TNFα down-regulates *TMEM182* transcript expression in adipocytes [28]. Its transcript expresses in white adipose tissues, heart, muscle, and lower relative levels of *TMEM182* transcript are found in kidney, testis, and brain. Identification of the intracellular signaling pathway involved in the TNFα-mediated decrease might be one clue offering insights into association between POAG and *TMEM182* function. Failure to confirm the association with POAG in the second stage could be attributable to clinical heterogeneity, but this result still needs to be confirmed in a second population. Nakano et al. demonstrated heterogeneity in the Japanese POAG population when their genome-wide association study of 1,575 Japanese POAG and normal subjects identified significant evidence of association with 6 SNPs on Chromosome 1, 10, 12 [29]. They did not report evidence of association with SNPs on Chromosome 2.

Table 5. Stage Two *NCK2* SNP rs2033008 Allele Frequencies in Japanese POAG, NTG and Controls Subjects.

	Allele frequency				Genotype			
	T	**A**	**Odds ratio (CI)**	**p value***	**T/T**	**T/A**	**A/A**	**p value****
POAG	0.703	0.297	0.87 (0.65–1.16)	0.35	89/187	85/187	13/187	0.069
NTG	0.750	0.250	0.69 (0.53–0.89)	0.0053	159/286	111/286	16/286	0.0056
Control	0.673	0.327			130/271	105/271	36/271	

*Fisher's exact test,
**Chi-square test.
A/A is mutant homozygote, T/A is heterozygote, and T/T is wild homozygote.
doi:10.1371/journal.pone.0054115.t005

Table 6. Correlation between the POAG or NTG Endophenotypes and *NCK2* SNP rs2033008 Screened in Stage Two.

Endophenotype	Age at diagnosis (y.o.)				Maximum IOP* (mmHg)				MD value of the visual field (dB)			
Genotype	**T/T**	**T/A**	**A/A**	**p value****	**T/T**	**T/A**	**A/A**	**p value****	**T/T**	**T/A**	**A/A**	**p value****
POAG	55.8	61.0	54.2	0.94	23.7	24.2	25.0	0.87	−15.38	−14.94	−12.28	0.63
NTG	56.8	56.0	52.2	0.70	16.7	17.0	16.0	0.79	−9.83	−10.95	−16.28	0.05

*IOP; intraocular pressure (under medication).
**Dunnett's test.
A/A is mutant homozygote, T/A is heterozygote, and T/T is wild homozygote.
doi:10.1371/journal.pone.0054115.t006

Thus these SNPs on Chr2 might be the variants for which our study is not well-powered, or clinical heterogeneity might be complicating our ability to detect the association in our limited sample size.

In our data set, *HK2* shows the strongest evidence of association with NTG in the Japanese population out of all of the genes that have SNPs represented on the screening panel we used.

Even when a single simple Mendelian locus causes a disease, variants in other genes may contribute to phenotypic variability, and phenotypic complexity along with locus and allele heterogeneity can complicate the problem of identifying the underlying causes of the disease. Our findings raise questions about whether additional genes in this region may be contributing to phenotypic heterogeneity within the NTG and POAG populations. The MD values of the visual field in these studies indicate middle to advanced stages of the disease, with the range of values possibly resulting from a combination of genetic complexity and genetic heterogeneity.

On the other hand, we also have to consider the importance of apparent gene deserts. The SNP rs1239066 shows significant evidence of association in both Stage One and Stage Two screenings, and in the meta-analysis (POAG, NTG; P = 0.001, 0.005). Significant evidence was also found for rs1027003 (POAG; P = 0,010) (Table 2), but neither one is in the immediate vicinity of a known gene. Wiggs et al. found significant evidence that genetic variants in a gene desert on 8q22 are associated with optic nerve damage in glaucoma [14]. So additional follow up studies will need to explore this gene desert region to determine whether any functional sequences there are playing a role in the disease.

Glaucoma is a complex disease, and it involves genetic variants that confer moderate to low effect sizes (e.g., OR = 1.2–1.5). The OR which was identified in the first stage with the P value cutoff of 0.01 was 1.68. This cutoff value was a bit strict to exclude the false positives.

Further investigations of the structure and function of the *HK2*, *NCK2* and *TMEM182* proteins would be helpful in understanding the pathogenesis of POAG and NTG. Our data suggest that *HK2* may play an important role in NTG in the Japanese population; although our data suggest that *HK2* might be the GLC1B gene, a firm conclusion on the subject awaits screening of members of the families originally used to map the GLC1B locus.

Patients and Methods

Ethics statement

This study was approved by the Institutional Review Board of Tohoku University, Keio University, Tokyo Metropolitan Police Hospital, Niigata University, Ideta Eye Hospital, and all procedures were conducted in accordance with the Declaration of Helsinki. All participants provided written informed consent after an explanation of the purpose and procedures to publish these case details.

Patient Recruitment and Characteristics

The samples used in the first screening (Stage One) were collected in Keio University hospitals, Tokyo Metropolitan Police Hospital, Niigata University, and Ideta Eye Hospital, and the

Table 7. Stage Two *TMEM182* SNP Allele Frequencies in Japanese POAG, NTG and Control Subjects.

	Allele frequency			Genotype			
rs869833	**A**	**G**	**p value***	**A/A**	**A/G**	**G/G**	**p value****
POAG	0.590	0.410	0.855	61/187	99/187	27/187	0.095
NTG	0.579	0.421	0.834	94/286	143/286	49/286	0.269
Control	0.585	0.415		100/271	117/271	54/271	
	Allele frequency			**Genotype**			
rs960011	**C**	**T**	**p value***	**C/C**	**C/T**	**T/T**	**p value****
POAG	0.503	0.497	0.363	45/187	98/187	44/187	0.479
NTG	0.520	0.480	0.641	76/286	145/286	65/286	0.782
Control	0.533	0.467		79/271	131/271	61/271	

*Fisher's exact test,
**Chi-square test.
G/G or T/T is mutant homozygote, A/G or C/T is heterozygote, and A/A or C/C is wild homozygote.
doi:10.1371/journal.pone.0054115.t007

Table 8. Correlation between the POAG or NTG Endophenotypes and *TMEM182* SNPs Screened in Stage Two.

Endophenotype	Age at diagnosis (y.o.)				Maximum IOP* (mmHg)				MD value of the visual field (dB)			
rs869833 Genotype	**A/A**	**A/G**	**G/G**	**p value****	**A/A**	**A/G**	**G/G**	**p value****	**A/A**	**A/G**	**G/G**	**p value****
POAG	54.8	61.1	56.0	0.95	24.7	23.8	23.3	0.80	−17.5	−15.0	−9.95	0.01
NTG	55.8	55.7	59.9	0.40	16.9	16.9	16.4	0.84	−12.60	−9.62	−12.21	0.98
rs960011Genotype	**C/C**	**C/T**	**T/T**	**p value****	**C/C**	**C/T**	**T/T**	**p value****	**C/C**	**C/T**	**T/T**	**p value****
POAG	55.5	57.3	62.0	0.29	24.8	24.4	23.2	0.73	−14.2	−18.5	−9.44	0.37
NTG	53.8	56.4	60.1	0.14	17.1	17.3	15.7	0.16	−10.77	−11.02	−11.76	0.88

*IOP; intra ocular pressure (under medication),
**Dunnett's test.
G/G or T/T is mutant homozygote, A/G or C/T is heterozygote, and A/A or C/C is wild homozygote.
doi:10.1371/journal.pone.0054115.t008

samples used in the second screening (Stage Two) were collected at Tohoku University.

Routine ophthalmic examinations were performed on all subjects. Individuals were included as POAG cases if they fulfilled the following inclusion criteria: 1) applanation IOP greater than 22 mm Hg in each eye; 2) spherical equivalent more than −8 diopter; 3) glaucomatous cupping in each eye including cup-to-disc ratio greater than 0.7; 4) visual field loss measured by Goldmann perimetry or Humphrey automated field analyzer (Carl Zeiss Meditec, Dublin, CA) in Stage One. The severity of the visual field defects was scored from 1 to 5 according to previously reported criteria ref. The data obtained by two types of perimetry were combined using a five-point scale: 1, no alterations; 2, early defects; 3, moderate defects; 4, severe defects; and 5, light perception only or no light perception. The first four groups on this severity scale followed Kozaki's classification based on Goldmann perimetry or the classification was based on results of Humphrey automated field analyzer [30,31]. Kozaki's classification is widely used in Japan. In Stage Two, all of the visual field loss were measured by Humphrey automated field analyzer according to Anderson-Pattela classification [30] consistent with the glaucomatous cupping in at least one eye; and 5) open anterior chamber angles; and exclusion of secondary causes (e.g., trauma, uveitis, or steroid-induced glaucoma). The criteria for NTG were the same as for POAG except that NTG subjects showed applanation IOP less than 22 mm Hg in both eyes at each examination. Baseline clinical parameters including age, gender, spherical equivalent base line visual acuity (VA), IOP measured by Goldmann applanation tonometry were recorded at the time of first diagnosis of POAG or NTG in each patient. Mean deviation (MD) values indicative of visual field damage were obtained by the Swedish interactive threshold algorithm (SITA)-standard strategy of the 30-2 program of HFA (Carl Zeiss Meditec, Dublin, Californuia, USA). MD was used on reliable visual field test results (<20% fixation errors, <33% false-positive results, and <33% false-negative results). Control subjects had these characteristics: IOP less than 22 mm Hg, normal optic discs, and no family history of glaucoma. To decrease the chance of enrolling individuals with pre-symp-

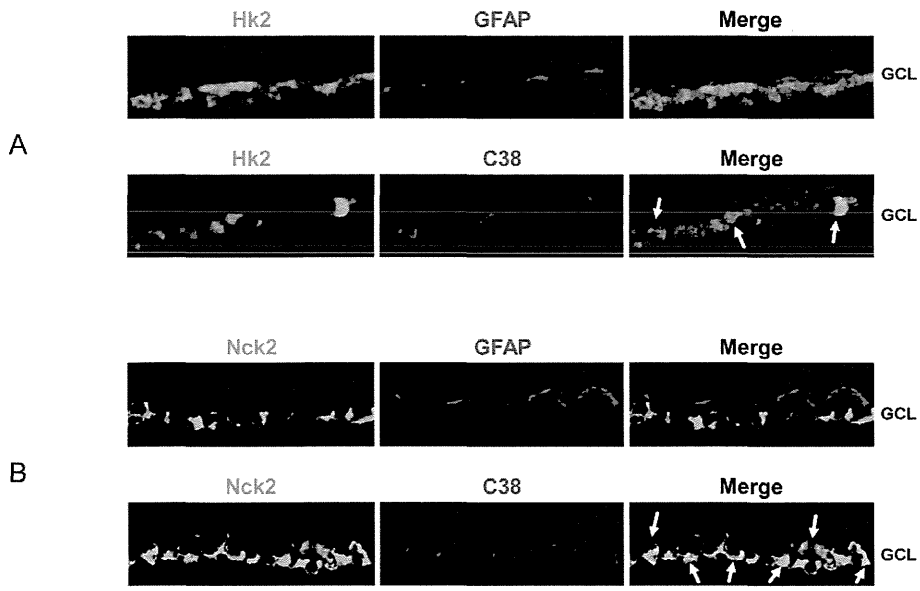

Figure 3. *Hk2* and *Nck2* Immunohistochemistory. Representative IHC photographs showing Hk2, Nck2, astrocyte maker (GFAP) and RGC marker (C38) in the retinas of untreated mice. Arrows indicated the co-localization area.
doi:10.1371/journal.pone.0054115.g003

tomatic glaucoma, we limited this group to individuals older than 60 years.

Two Stage Screening Protocol

The two-stage screening strategy is shown in Figure 1. The first stage screened used 669 SNPs from the GLC1B region, using the Illumina panel #8 (Chromosome 2; 77–117 Mbp) (Illumina, San Diego, CA, USA) carried by Illumina (San Diego, CA, USA), and each SNP was tested for association with POAG or NTG. The first stage used a cohort of 368 unrelated Japanese individuals: 123 POAG cases (63 men and 60 women), 121 NTG cases (61 men and 60 women) and 120 normal subjects (61 men and 59 women). Mean age of POAG cases was 56.9±11.5 years. Mean age of NTG cases was 54.0±12.3 years. Mean age of controls was 70.3±10.2 years. The visual field scores were 2.8±1.0 in POAG cases and 2.7±0.9 in NTG cases (Table 9). Single-nucleotide polymorphisms (SNPs) with a call rate <90% were excluded from the analysis. All of the polymorphisms showed no deviation from Hardy–Weinberg equilibrium ($P>0.05$) except rs2033008 in Stage One ($p = 0.030$).

The second stage screened SNPs that showed significant evidence for association in the first round in this study ($p<0.01$) and in the NCK2 gene, which previously showed association with NTG [16]. The odds ratio which was identified in the first stage with the P value cutoff of 0.01 was 1.68. Second stage screening was carried out using sequencing of DNA PCR amplified by polymerase chain reaction from genomic DNA samples from a population of 473 unrelated Japanese individuals, including 187 POAG cases (119 men and 68 women), 286 cases NTG (139 men and 147 women), and 271 control subjects (145 men and 126 women). Mean age of POAG cases was 57.8±12.0 years. Mean age of NTG cases was 56.4±13.3years. Mean age of controls was 69.7±9.3 years. Maximum intra ocular pressure under medication were 23.5±5.3 mmHg in POAG subjects and 16.8±2.4 mmHg in NTG subjects. Mean deviation (MD) value of the visual field test was −15.0±9.0 dB in POAG cases and −11.0±7.1 dB in NTG cases (Table 9).

Sample Preparation

Genomic DNA was extracted from leukocytes of the peripheral blood. It was purified by the Qiagen QIAamp Blood Kit (Qiagen, Valencia, CA, USA).

Mutation Screening

Mutation screening was carried out in genes that contained SNPs that showed significant evidence of association in the first stage (HK2 and TMEM182) plus the previously-reported NCK2 gene [16]. All of the exons of the *HK2*, *NCK2*, *TMSB10* and *TMEM182* genes, and positive SNPs were amplified by a polymerase chain reaction (PCR) using 0.5 μM concentration of primers in an amplification mixture (25 μl) containing 0.2 mM dNTPs and 0.5 U Ex Taq polymerase (Takara Bio, Shiga, Japan) with 30 ng template DNA. Oligonucleotides for amplification and sequencing were selected using Primer3 software (http://frodo.wi.mit.edu/cgi-bin/primer3/primer3_www.cgi/ provided in the public domain by the Massachusetts Institute of Technology, Cambridge, MA). Primers for amplification and sequencing of coding sequence were placed in introns far enough from the intron/exon junctions to allow for visualization of the splice site sequences. The PCR fragments were purified with ExoSAP-IT (USB, Cleveland, Ohio, USA), sequenced by the BigDye™ Terminator v3.1 Cycle Sequencing Kit (Perkin-Elmer, Foster City, CA, USA) on an automated DNA sequencer (ABI PRISM™ 3100 Genetic Analyzer, Perkin-Elmer, Waltham, MA, USA).

Statistical Analysis

The significance of association was determined by contingency table analysis using Fisher's exact test or Chi-square test, depending on cell counts. In estimation of genotype-phenotype correlation, we used Dunnett's test to compare group means of those carrying the mutant variant being tested against the group means of those carrying the normal, reference sequence. Odds ratios (approximating to relative risk) were calculated as a measure of the association between the allele frequency and the phenotype of POAG/NTG, estimated using the SNPAlyze program version 7.0 (Dynacom, Yokohama, Japan). Hardy–Weinberg equilibrium was analyzed using gene frequencies obtained by simple gene counting and the chi-square test with Yates' correction for comparing observed and expected values.

Immunohistochemistory of the *HK2* and *NCK2*

Murine retinas were fixed with 4% PFA at 4°C overnight and then cryoprotected in phosphate buffered saline (PBS) with 20% sucrose. Cryosections (thickness 10 μm) were mounted on the slides and incubated with blocking buffer (10% goat serum, 0.5% gelatin, 3% BSA and 0.2% Tween 20 in PBS). Next, they were incubated with primary antibodies at 4°C overnight. Primary

Table 9. Clinical Characteristics of Subjects studied in Stage One and Two Screening.

Endophenotype		Age at diagnosis (y.o.)	Maximum IOP* (mmHg)	The Visual Field Score**
Stage One	POAG	56.9±11.4	25.3±5.6	2.8±1.0
	NTG	54.0±12.2	16.0±2.3	2.7±0.9
	Control	70.3±10.2	13.9±2.2	
Stage Two	POAG	57.8±12.0	23.5±5.3	−15.0±9.0 (dB)
	NTG	56.4±13.3	16.8±2.4	−11.0±7.1 (dB)
	Control	69.7±9.3	13.9±2.2	

*IOP; intra ocular pressure (under medication).

**The Visual Field Score was evaluated by Humphrey MD value or Goldmann perimetry (Stage One) and Humphrey MD value (Stage Two).

In Stage One, the severity of the visual field defects was scored from 1 to 5 according to previously reported criteria. The data obtained by two types of perimetry were combined using a five-point scale: 1, no alterations; 2, early defects; 3, moderate defects; 4, severe defects; and 5, light perception only or no light perception. The first four groups on this severity scale followed Kozaki's classification based on Goldmann perimetry or the classification was based on results of visual field perimetry (Humphrey Field Analyzer; Carl Zeiss Meditec, Dublin, CA). Kozaki's classification is widely used in Japan.

doi:10.1371/journal.pone.0054115.t009

antibodies used were Mouse anti-Glial Fibrillary Acidic Protein (GFAP) (1:200; MAB360; Chemicon, Millipore, MA, USA), mouse anti-C38 (1:200; provided by Dr. Jun Kosaka), rabbit anti-NCK2 (1:200; ab14590; Abcam), or rabbit anti-HK2 (1:200; 2867S; Cell Signaling Technology, MA, USA). The sections were washed three times with PBST (PBS containing 0.2% Tween 20) and then incubated with secondary goat anti-rabbit IgG antibody (1:200; A11008 Invitrogen, Carlsbad, CA, USA) tagged with Alexa 488 or goat anti-mouse IgG A11030; Invitrogen, Carlsbad, CA, USA) tagged with Alexa 546 for 1 hour. The slides were washed three times and mounted with Vectashield mounting medium (H1000; Vector, Burlingame, CA).

Acknowledgments

The authors thank Dr. Duco I. Hamasaki for editing the manuscript, and thank Dr. Nariyuki Yamada and Prof. Makoto Tamai for experimental suggestions and support. We are grateful to Dr. Jun Kosaka for providing antibody mouse anti-C38.

Author Contributions

Conceived and designed the experiments: T. Funayama YM KN NF. Performed the experiments: DS T. Funayama YT AS KY MM AM TN NF. Analyzed the data: DS T. Funayama YM JER NF. Contributed reagents/materials/analysis tools: T. Funayama YT AS NY T. Fukuchi HA HI TN. Wrote the paper: DS KY JER NF.

References

1. Quigley H (1996) Number of people with glaucoma worldwide. Br J Ophthalmol 80: 389–393.
2. Quigley H (1993) Open-angle glaucoma. N Engl J Med 328: 1097–1106.
3. Hitchings RA, Anderton SA (1983) A comparative study of visual field defects seen in patients with low-tension glaucoma and chronic simple glaucoma. Br J Ophthalmol 67: 818–821.
4. Hitchings R (1992) Low tension glaucoma–its place in modern glaucoma practice. Br J Ophthalmol 76: 494–496.
5. Werner E (1996) Normal-tension glaucoma.; Ritch R SM, Krupin T, eds., editor. St.Louis: Mosby. 769–797 p.
6. Shiose Y, Kitazawa Y, Tsukahara S, Akamatsu T, Mizokami K, et al. (1991) Epidemiology of glaucoma in Japan–a nationwide glaucoma survey. Jpn J Ophthalmol 35: 133–155.
7. Iwase A, Suzuki Y, Araie M, Yamamoto T, Abe H, et al. (2004) The prevalence of primary open-angle glaucoma in Japanese: the Tajimi Study. Ophthalmology 111: 1641–1648.
8. Raymond V (1997) Molecular genetics of the glaucomas: mapping of the first five "GLC" loci. Am J Hum Genet 60: 272–277.
9. Sarfarazi M (1997) Recent advances in molecular genetics of glaucomas. Hum Mol Genet 6: 1667–1677.
10. Liu Y, Allingham RR (2011) Molecular genetics in glaucoma. Exp Eye Res 93: 331–339.
11. Pasutto F, Keller KE, Weisschuh N, Sticht H, Samples JR, et al. (2012) Variants in ASB10 are associated with open-angle glaucoma. Hum Mol Genet 21: 1336–1349.
12. Burdon KP, Macgregor S, Hewitt AW, Sharma S, Chidlow G, et al. (2011) Genome-wide association study identifies susceptibility loci for open angle glaucoma at TMCO1 and CDKN2B-AS1. Nat Genet 43: 574–578.
13. Ramdas WD, van Koolwijk LM, Lemij HG, Pasutto F, Cree AJ, et al. (2011) Common genetic variants associated with open-angle glaucoma. Hum Mol Genet 20: 2464–2471.
14. Wiggs JL, Yaspan BL, Hauser MA, Kang JH, Allingham RR, et al. (2012) Common variants at 9p21 and 8q22 are associated with increased susceptibility to optic nerve degeneration in glaucoma. PLoS Genet 8: e1002654.
15. Stoilova D, Child A, Trifan OC, Crick RP, Coakes RL, et al. (1996) Localization of a locus (GLC1B) for adult-onset primary open angle glaucoma to the 2cen-q13 region. Genomics 36: 142–150.
16. Akiyama M, Yatsu K, Ota M, Katsuyama Y, Kashiwagi K, et al. (2008) Microsatellite analysis of the GLC1B locus on chromosome 2 points to NCK2 as a new candidate gene for normal tension glaucoma. Br J Ophthalmol 92: 1293–1296.
17. Laakso M, Malkki M, Deeb SS (1995) Amino acid substitutions in hexokinase II among patients with NIDDM. Diabetes 44: 330–334.
18. Laakso M, Malkki M, Kekalainen P, Kuusisto J, Deeb SS (1995) Polymorphisms of the human hexokinase II gene: lack of association with NIDDM and insulin resistance. Diabetologia 38: 617–622.
19. Vidal-Puig A, Printz RL, Stratton IM, Granner DK, Moller DE (1995) Analysis of the hexokinase II gene in subjects with insulin resistance and NIDDM and detection of a Gln142–>His substitution. Diabetes 44: 340–346.
20. Echwald SM, Bjorbaek C, Hansen T, Clausen JO, Vestergaard H, et al. (1995) Identification of four amino acid substitutions in hexokinase II and studies of relationships to NIDDM, glucose effectiveness, and insulin sensitivity. Diabetes 44: 347–353.
21. da-Silva WS, Gomez-Puyou A, de Gomez-Puyou MT, Moreno-Sanchez R, De Felice FG, et al. (2004) Mitochondrial bound hexokinase activity as a preventive antioxidant defense: steady-state ADP formation as a regulatory mechanism of membrane potential and reactive oxygen species generation in mitochondria. J Biol Chem 279: 39846–39855.
22. Santiago AP, Chaves EA, Oliveira MF, Galina A (2008) Reactive oxygen species generation is modulated by mitochondrial kinases: correlation with mitochondrial antioxidant peroxidases in rat tissues. Biochimie 90: 1566–1577.
23. Majewski N, Nogueira V, Bhaskar P, Coy PE, Skeen JE, et al. (2004) Hexokinase-mitochondria interaction mediated by Akt is required to inhibit apoptosis in the presence or absence of Bax and Bak. Mol Cell 16: 819–830.
24. Inagaki Y, Mashima Y, Fuse N, Ohtake Y, Fujimaki T, et al. (2006) Mitochondrial DNA mutations with Leber's hereditary optic neuropathy in Japanese patients with open-angle glaucoma. Jpn J Ophthalmol 50: 128–134.
25. Buday L, Wunderlich L, Tamas P (2002) The Nck family of adapter proteins: regulators of actin cytoskeleton. Cell Signal 14: 723–731.
26. Suzuki S, Mizutani M, Suzuki K, Yamada M, Kojima M, et al. (2002) Brain-derived neurotrophic factor promotes interaction of the Nck2 adaptor protein with the TrkB tyrosine kinase receptor. Biochem Biophys Res Commun 294: 1087–1092.
27. Harada C, Guo X, Namekata K, Kimura A, Nakamura K, et al. (2011) Glia- and neuron-specific functions of TrkB signalling during retinal degeneration and regeneration. Nat Commun 2: 189.
28. Wu Y, Smas CM (2008) Expression and regulation of transcript for the novel transmembrane protein Tmem182 in the adipocyte and muscle lineage. BMC Res Notes 1: 85.
29. Nakano M, Ikeda Y, Taniguchi T, Yagi T, Fuwa M, et al. (2009) Three susceptible loci associated with primary open-angle glaucoma identified by genome-wide association study in a Japanese population. Proc Natl Acad Sci U S A 106: 12838–12842.
30. Anderson DR, VM P (1999) Automated Static Perimetry. 2nd edition. St.Louis: Mosby.
31. Funayama T, Ishikawa K, Ohtake Y, Tanino T, Kurosaka D, et al. (2004) Variants in optineurin gene and their association with tumor necrosis factor-alpha polymorphisms in Japanese patients with glaucoma. Invest Ophthalmol Vis Sci 45: 4359–4367.

Effect of Topical Tafluprost on Optic Nerve Head Blood Flow in Patients With Myopic Disc Type

Satoru Tsuda, MD, Yu Yokoyama, MD, Naoki Chiba, MD, Naoko Aizawa, MD, Yukihiro Shiga, MD, Masayuki Yasuda, MD, Shunji Yokokura, PhD, MD, Takaaki Otomo, MD, Nobuo Fuse, PhD, MD, and Toru Nakazawa, PhD, MD

Purpose: To investigate the effect of topical tafluprost on optic disc blood flow in patients with myopic disc.

Materials and Methods: Forty-eight eyes in 24 patients with a myopic disc type (oval shaped) optic disc tilted to the temporal, with a crescent peripapillary atrophy were included in this study. Twenty-eight eyes were diagnosed as normal tension glaucoma and 20 eyes were in normal subjects. None had any treatment for glaucoma. Average age was 45.3 ± 11.9 years. One eye was treated with topical tafluprost and the fellow eye served as the control. Ocular blood flow was measured by laser speckle flowgraphy (LSFG-NAVI) at 30, 60, 90, and 120 minutes after tafluprost administration, and the mean blur rate (MBR) on the optic disc was analyzed. Blood pressure and intraocular pressure (IOP) were recorded.

Results: In all subjects, topical tafluprost (a) significantly reduced IOP versus baseline from 60 minutes after treatment (baseline: 15.2 ± 3.4 mm Hg, 60 min: 13.3 ± 3.2 mm Hg, $P = 0.001$, 90 min: 13.3 ± 3.6 mm Hg, $P = 0.002$, 120 min: 13.7 ± 3.4 mm Hg, $P = 0.007$); and (b) significantly increased the MBR versus baseline (60 min: + 4.3 ± 6.6%, $P = 0.008$, 90 min: + 5.0 ± 4.9%, $P < 0.001$, 120 min: + 6.7 ± 7.0%, $P < 0.001$).

Conclusions: Topical tafluprost increased MBR in the optic nerve head and significantly reduced IOP, effects that may represent beneficial treatment for glaucoma patients with a myopic disc type.

Key Words: blood flow, prostaglandin F2-α, normal tension glaucoma, myopia

(*J Glaucoma* 2013;22:398–403)

Ocular blood flow is thought to be a risk factor in the pathology of glaucoma, alongside intraocular pressure (IOP),[1–4] and a compromised local ocular blood flow may lead to visual-field deterioration. Since fluorescein angiography has revealed a filling defect in the optic nerve head (ONH) in patients with glaucoma,[5–9] an induced improvement in ocular blood flow may be an effective form of glaucoma treatment.

In our recent publication, 20% of the patients with glaucoma exhibited a decreased best corrected visual acuity (BCVA: < 20/20) due to glaucoma[10] and those patients with a severe by decreased BCVA (< 0.3) had a myopic disc type.[10] Furthermore, our hospital-based retrospective study on the advanced stage of normal tension glaucoma (NTG) revealed that a significant number of severe NTG patients had the myopic disc type.[11] When our fluorescein angiography study detected a filling defect in the temporal area of the tilted myopic disc,[10] we were motivated to investigate the ocular circulation, especially in glaucoma patients with a myopic disc type.

Ocular blood flow may be measured using the Heidelberg Retina Flowmeter,[12] color Doppler imaging,[13] laser speckle flowgraphy (LSFG),[14–17] or laser Doppler velocimetry.[18] LSFG, a noninvasive technique that can measure relative ONH blood flow using the laser speckle phenomenon,[15] is often employed to investigate the effect of glaucoma eye drops on the ocular circulation.[19] Recently, LSFG-NAVI, a newer version of LSFG, became commercially available, and in this machine the focusing of the acquired image is significantly improved. The intrasession reproducibility of mean blur rate (MBR) in ONH was excellent (coefficient of variation, 3.4 ± 2.0%).[20]

In Asia, the major type of glaucoma is NTG, not high-pressure glaucoma,[21] and there is a limitation to the lowering of IOP in patients with NTG.[22] A recently, excellent review on ocular blood flow suggested that a decreased ocular circulation is related to the prevalence and progression of glaucoma.[23] However, there is no published evidence that treatment aimed at restoring the ocular circulation can impede the progression of glaucoma, despite several studies investigating the increases in ONH blood flow achieved with clinically used topical antiglaucoma eye drops.[19,24,25] Tafluprost represents a new generation of potent FP-receptor agonists[26] and 2 recent studies of the effect of tafluprost instillation on ONH blood flow have reported vascular dilation during endothelin-1-induced arterial vessel constriction in an ex vivo rabbit experiment[27] and in monkeys in vivo.[28] We hypothesized that topical tafluprost might not only lower IOP, but also improve the ocular circulation in patients with NTG.

Therefore, in this study we investigated the effect of topical tafluprost on ONH blood flow using LSFG-NAVI both in glaucoma patients and in normal volunteers with the myopic disc type. We instilled topical tafluprost into only 1 eye, the fellow eye serving as control, and we compared the ocular blood flow in the ONH with the baseline value every 30 minutes until 120 minutes after the instillation.

MATERIALS AND METHODS

Eligibility of Participants

Forty-eight eyes in 24 participants with a myopic disc type (oval shaped) optic disc tilted to the temporal, with a

Received for publication February 23, 2011; accepted September 12, 2011.
From the Department of Ophthalmology, Tohoku University Graduate School of Medicine, Aoba-ku, Sendai, Miyagi, Japan.
Disclosure: The authors declare no conflict of interest.
Reprints: Toru Nakazawa, PhD, MD, Department of Ophthalmology, Tohoku University Graduate School of Medicine, 1-1 Seiryo-machi, Aoba-ku, Sendai, Miyagi 980-8574, Japan (e-mail: ntoru@oph.med.tohoku.ac.jp).

DOI:10.1097/IJG.0b013e318237c8b3

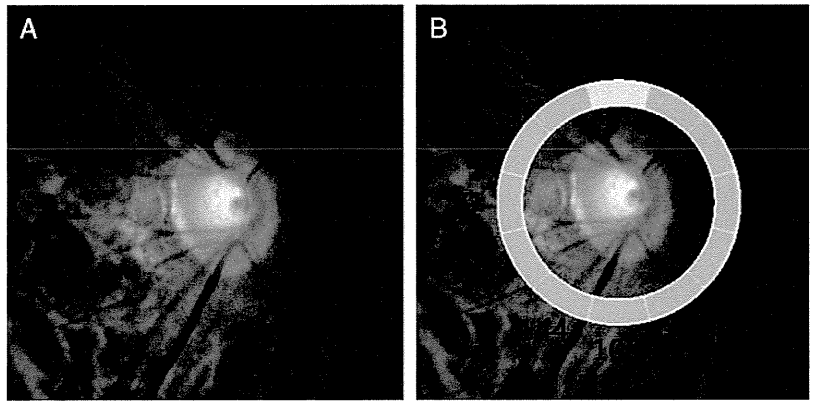

FIGURE 1. A, The fundus photograph shows a typical myopia-type optic disc. The optic disc is oval, is tilted to temporal side with crescent peripapillary atrophy. B, The colored circle and thickness (μm) on the fundus photograph showed retinal nerve fiber layer thickness. This patient had thin retinal nerve fiber layer in the 12 o'clock position.

crescent peripapillary atrophy were included in this study (Fig. 1A). The optic disc shape and condition was determined by the fundus photograph and retinal nerve fiber layer thickness around a optic disc obtained using 3-dimensional OCT-1000 (Topcon Corporation, Tokyo, Japan) (Fig. 1B). The participating group comprised of 28 eyes belonging to 14 glaucoma patients (age 52.3 ± 9.7; 37 to 70 y; male/female: 7/7) and 20 eyes in 10 healthy volunteers (age 35.5 ± 6.6; 25 to 42 y; male/female: 9/1). The glaucoma patients were under observation at our department of ophthalmology, and gave written informed consent to their participation in this study. This study followed the Tenets of the Declaration of Helsinki, and the institutional review board of Tohoku University approved the consent forms for this study. None of the 24 participants had previously had any antiglaucoma eye drops instilled, nor were any of them on any systemic medications that could alter the ocular blood flow, such as Ca^{2+}-channel blockers or β-blockers. Participants were excluded if: ocular diseases other than open-angle glaucoma were present, systemic diseases affecting the visual fields were present, they had undergone intraocular surgery, or their spherical equivalent was < -8 D. BCVA was measured using a standard Japanese decimal visual acuity chart, and the values were converted to logMAR units. IOP was measured by Goldmann applanation tonometry.

Administration of Topical Tafluprost

Tafluprost (TAPROS; Santen Pharmaceutical, Osaka, Japan) is a selective FP agonist with an IOP-lowering effect. It was recently reported that tafluprost improved the microcirculation in the healthy human ONH.[29] In each subject, 1 drop of 0.0015% tafluprost was instilled once into the eye that had the higher IOP or in which visual-field loss was more advanced. The fellow eye served as control. If the pupils of a given participant were too small to allow measurement of blood flow using LSFG-NAVI, 0.4% tropicamide (Mydrin M; Santen Pharmaceutical) was instilled into both the eyes. The IOP, ONH blood flow, blood pressure, and pulse rate were measured before treatment (0), and at 30, 60, 90, and 120 minutes after instillation of tafluprost. For those measurements, we used Goldmann applanation and an automated sphygmomanometer. Mean blood pressure was calculated from the blood pressure values, and ocular perfusion pressure (OPP) was calculated using the formula OPP = 2/3 mean blood pressure − IOP.

Diagnosis of Glaucoma

Glaucoma was diagnosed by the cupping of the optic disc and the corresponding visual-field loss. Automated perimetry was performed using a Humphrey Field Analyzer (SITA standard program 30-2). Reliability criteria included fixation losses, and false-positive and false-negative rates of $< 20\%$. Twenty-eight eyes had glaucomatous visual-field loss according to the Anderson-Pattela classification, as follows: (1) the Glaucoma Hemifield Test was outside normal limits; (2) there was a cluster of ≥ 3 nonedge points in a location typical of glaucoma, all of which were depressed on the pattern deviation plot at the $P < 5\%$ level and one of which was depressed at the $P < 1\%$ level; (3) the corrected pattern SD was significant at the $P < 5\%$ level.

LSFG

The effects of topical tafluprost instillation on ONH blood flow were studied using the MBR, a blood-flow parameter in LSFG. The MBR was calculated from the blood-flow map obtained using analysis software provided for LSFG (LSFG analyzer, version 3.0.20.0). After we had identified the margin of the optic disc using an ellipsoidal band by manually, all the positions were saved and used on the same patient for subsequent analyses automatically. The ONH area on the blood-flow map was determined by fitting on ellipsoidal rubber band to the borderline of the ONH. Consecutive MBR measurements were performed 3 times to get an average MBR for each time-point. The changes in MBR were normalized to the baseline value (last measurement before topical tafluprost instillation), and normalized values were compared between the treatment eyes and the fellow control eyes in the same patients.

Statistical Analysis

A paired t test was used to examine differences from the baseline, and repeated-measures analysis of variance and a paired t test were applied to the difference between the 2 eyes. When necessary, Bonferroni correction was used to adjust P values. $P < 0.05$ was considered significant.

TABLE 1. Changes in Ocular and Systemic Parameters With Time in All Participants (n = 24)

All Participants	Pretreatment Value	30 min	60 min	90 min	120 min
IOP (mm Hg)					
Treatment eyes	15.2 ± 3.4	14.5 ± 2.9	13.3 ± 3.2†	13.3 ± 3.6†	13.7 ± 3.4†
Control eyes	14.9 ± 3.5	14.7 ± 3.0	14.3 ± 3.0	13.8 ± 3.2	14.1 ± 3.0
ONH blood flow (% MBR)					
Treatment eyes	100.0 ± 0	103.3 ± 6.8	104.3 ± 6.6†	105.0 ± 4.9†	106.7 ± 7.0†
Control eyes	100.0 ± 0	101.2 ± 4.0	101.3 ± 5.8	102.9 ± 5.3	103.5 ± 7.7
OPP (mm Hg)					
Treatment eyes	47.1 ± 5.3	44.5 ± 6.4	45.8 ± 7.4†	44.8 ± 5.9	45.3 ± 5.3
Control eyes	47.5 ± 5.4	44.3 ± 6.3*	44.9 ± 7.0*	44.3 ± 5.8†	45.1 ± 5.2
MBP (mm Hg)	93.6 ± 10.7	88.4 ± 12.5†	88.7 ± 13.2†	87.0 ± 10.4†	88.5 ± 10.5†
Pulse rate (/min)	76.5 ± 11.2	73.5 ± 9.2	72.0 ± 10.4†	70.6 ± 9.2†	69.2 ± 8.3†

Data showed the mean ± SD.
*$P < 0.05$ (Bonferroni correction vs. baseline value).
†$P < 0.01$ (Bonferroni correction vs. baseline value).
IOP indicates intraocular pressure; MBP, mean blood pressure; MBR, mean blur rate; ONH, optic nerve head; OPP, ocular perfusion pressure.

RESULTS

In all the tafluprost-treatment eyes (hereafter called "treatment eyes"), ONH blood flow (% MBR) reached its maximum increase during the study period (6.7% vs. baseline) at 120 minutes after the tafluprost instillation (Table 1, Figs. 2, 3). The change was significant at 60, 90, and 120 minutes ($P = 0.008$, < 0.001, and < 0.001, respectively; Bonferroni correction). In contrast, in all control eyes no significant difference versus baseline was observed at the any time-point. Overall, there was a difference in ONH blood flow changes between all treatment eyes and all control eyes ($P < 0.001$).

In all treatment eyes, the maximum decrease in IOP was by 1.9 mm Hg versus baseline at 60 minutes after the tafluprost instillation (Fig. 4). The change in IOP was significant at 60, 90, and 120 minutes ($P = 0.001$, 0.002, 0.007, respectively; Bonferroni correction). In all control eyes, IOP decreased significantly versus baseline only at 90 minutes ($P = 0.044$; Bonferroni correction). Overall, there was a significant difference in IOP between all treatment eyes and all control eyes ($P < 0.01$).

In those treatment eyes with glaucoma, ONH blood flow showed a maximum increase during the study period of 6.5% versus baseline at 120 minutes after the tafluprost instillation (Fig. 5). The change was significant at 90 and 120 minutes ($P = 0.025$, 0.049, respectively; Bonferroni correction). In glaucoma control eyes, a significant difference versus baseline was observed only at 90 minutes. Overall, a significant difference was seen in ONH blood flow changes between treatment eyes and control eyes in the glaucoma group ($P < 0.01$).

In those treatment eyes with glaucoma, IOP exhibited a maximum decrease of 2.5 mm Hg versus baseline at 60 minutes after the tafluprost instillation (Fig. 6). The change in IOP was significant at 60 to 90 minutes ($P = 0.001$, 0.023, respectively; Bonferroni correction). In glaucoma control eyes, there was no significant difference versus baseline at the any time-point, and overall there was

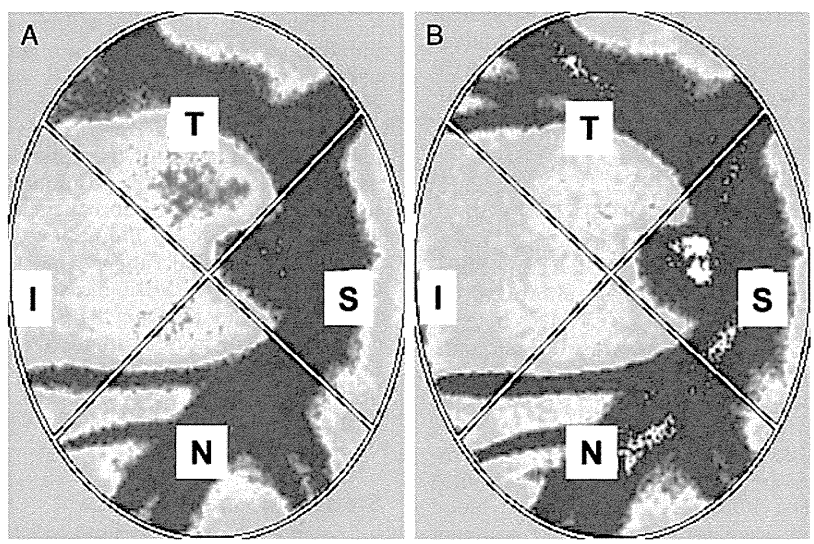

FIGURE 2. Comparisons of average mean blur rate (MBR) of the entire optic disc area between before and after the administration of tafluprost in the treatment eye with glaucoma. A, The blood-flow map of the optic disc area before the administration of tafluprost. The value of MBR is 22.3. B, The blood-flow map of the optic disc area at 120 minutes after the administration of tafluprost. The value of MBR is 27.8.

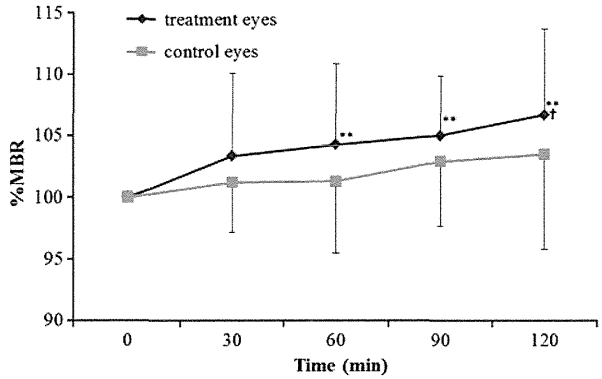

FIGURE 3. Changes in rate of optic nerve head blood flow versus baseline in all treatment eyes and control eyes. Data showed the mean ± SD. *P<0.05, **P<0.01 (Bonferroni correction vs. baseline value). MBR indicates mean blur rate.

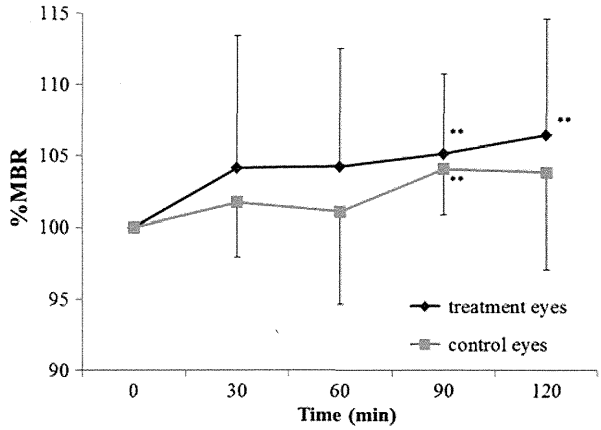

FIGURE 5. Changes in rate of optic nerve head blood flow versus baseline in those treatment eyes with glaucoma and their control eyes. Data showed the mean ± SD. *P<0.05, **P<0.01 (Bonferroni correction vs. baseline value). MBR indicates mean blur rate.

a significant difference in IOP between glaucoma treatment eyes and their control eyes (P < 0.01).

In all participants, mean blood pressure was significantly lower than baseline at 30 to 120 minutes after instillation of tafluprost, and pulse rate was significantly decreased versus baseline at 60 to 120 minutes (Table 1). In glaucoma patients, mean blood pressure was significantly lower than baseline at 90 minutes after instillation of tafluprost, and pulse rate was significantly decreased versus baseline at 120 minutes (Table 2).

OPP did not change significantly in all treatment eyes, but it was significantly below baseline in all control eyes at 30 to 90 minutes (Table 1). In glaucoma patients, OPP did not change significantly in treatment and control eyes (Table 2).

DISCUSSION

In this study, we found that topical administration of tafluprost significantly reduced IOP and increased ONH blood flow both in the normal volunteers and in the NTG patients with a myopic disc type. Significance was established at 60 minutes after its administration and the effects were still present at 120 minutes. These data suggest that topical tafluprost may be beneficial not only in lowering IOP, but also in improving the ocular circulation in NTG patients with a myopic disc type.

In this study, LSFG-NAVI was used to evaluate ONH blood flow. With this technique, normalized blur, square blur rate, and MBR values can be used as indicators of blood flow.[14,17,30–32] MBR, as used in the present study, is a new parameter in a LSFG-NAVI, an improved version of LSFG available from 2008. In a LSFG-NAVI, the ability of the system to focus so as to capture the speckle images is significantly improved, and a wider field of view and a higher resolution are used to generate the blood-flow map than in the previous version of LSFG.[31,32] LSFG-NAVI thereby enabled us to detect even modest eye drop-induced changes in ONH blood flow in humans. These improvements suggest that LSFG-NAVI has good potential in clinical use as a way to assess blood flow in patients with ocular diseases.

In the present study, topical administration of tafluprost significantly increased ONH blood flow both in the normal volunteers and in the NTG patients. Previous data have demonstrated that topical application of tafluprost

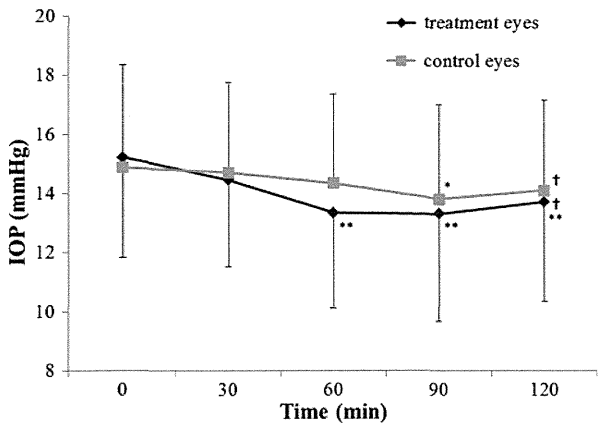

FIGURE 4. Changes in intraocular pressure (IOP) with time in all treated eyes and control eyes. Data showed the mean ± SD. *P<0.05, **P<0.01 (Bonferroni correction vs. baseline value).

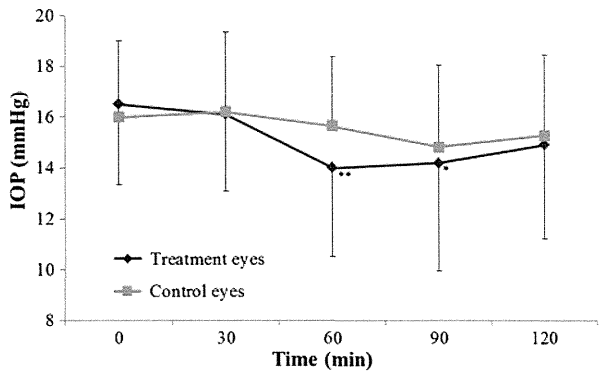

FIGURE 6. Changes in intraocular pressure (IOP) with time in those treatment eyes with glaucoma and their control eyes. Data showed the mean ± SD. *P<0.05, **P<0.01 (Bonferroni correction vs. baseline value).